Magnetoencephalography to Image the Acute Modulation of Brain Activity by Spinal Cord Stimulation Treatment in Chronic Pain Patients

MSc Thesis by Lucas Ottenheym

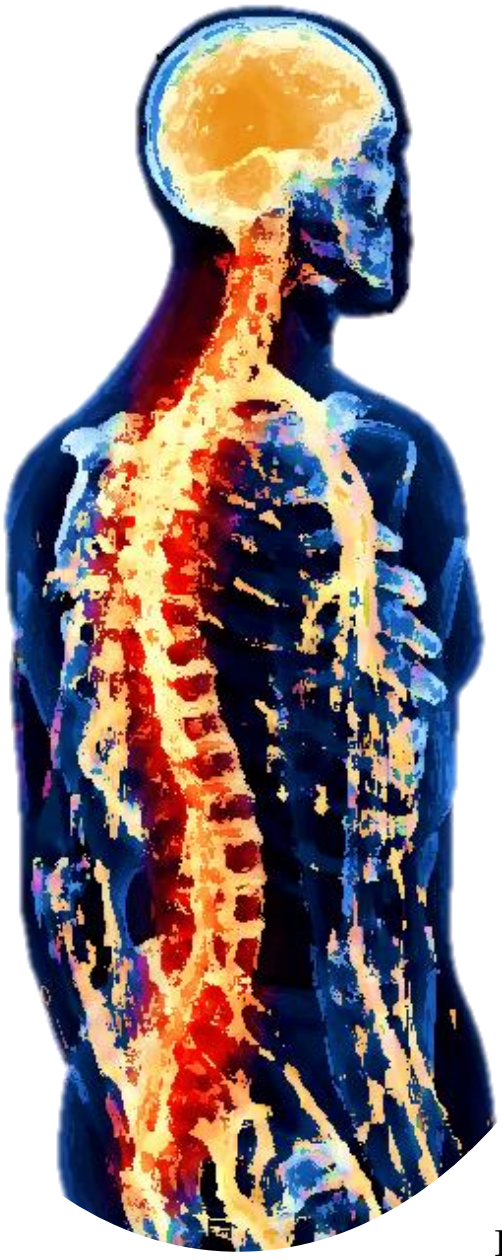

Supervised by
Dr. ir. C.C. de Vos
Dr. S.P.G. Frankema
B. Witjes, MSc

Universiteit Leiden
TU Delft Delft University of Technology
Erasmus Universiteit Rotterdam

Magnetoencephalography to image the acute modulation of brain activity by spinal cord stimulation treatment in chronic pain patients

Lucas Ottenheym

Student number : 4306651

23rd of April 2021

Thesis in partial fulfilment of the requirements for the joint degree of Master of Science in

Technical Medicine

Leiden University | Delft University of Technology | Erasmus University Rotterdam

Master thesis project (TM30004; 35 ECTS)

Center for Pain Medicine, Erasmus MC

October 2020 – April 2021

Supervisors:
Dr. ir. C.C. de Vos
Dr. S.P.G. Frankema
B. Witjes, MSc

Thesis committee member:
Prof. dr. ir. Jaap Harlaar, TU Delft (chair)

Contents

Abstract

Background: Spinal cord stimulation (SCS) is a last resort therapy for chronic pain syndromes, of which the exact mechanisms of action remain unknown. Although often effective, not all patients have sufficient pain reduction after implantation.

Objective: Analyse the acute effects of tonic and burst SCS on spectral features in the whole brain and in specific brain regions using magnetoencephalography (MEG).

Methods: Resting state MEG recordings of seventeen patients with SCS set to a cyclic stimulation program were analysed. Spectral analysis was done by computing power spectrum densities and calculating the ratio between different frequency bands. Time frequency decompositions were then computed to image the spectral changes over time.

Results: I showed a shift of power to the 7-10 Hz range during tonic and burst stimulation ON, and that burst stimulation modulated the regions involved in the medial pathway more than tonic stimulation did. I also hypothesised that burst stimulation has a lingering effect on the neuronal activity after it is switched OFF. Lastly, I showed that alpha power decreased at the moment the stimulation switched ON or OFF.

Conclusion: Although most findings were not statistically significant, the results were similar to the results of studies with patients who had longer exposure to SCS. There is still room for improvement in SCS treatment, and MEG analysis of acute modulation can help to gain more insight in its working mechanisms.

Abbreviations

AAL	automated anatomical labelling
AIC	anterior insular cortex
CRPS	chronic regional pain syndrome
dACC	dorsal anterior cingulate cortex
dlPFC	dorsolateral prefrontal cortex
ECG	electrocardiogram
EEG	electroencephalography
EOG	electrooculogram
FBSS	failed back surgery syndrome
MDT	medial dorsal thalamus
MEG	magnetoencephalography
NRS	numeric rating scale
PCA	principle component analysis
PSD	power spectral density
S1	primary sensory cortex
SCS	spinal cord stimulation
SSPs	signal-space projections
TF	time-frequency
TFD	time-frequency decomposition
V1	primary visual cortex

1. Introduction

1.1 Chronic pain

From drinking coffee that is still too hot to bumping your toe, the sensation of pain is an everyday phenomenon, but meanwhile remains a subject of scientific debate. As recent as September 2020 the definition of pain has been revised by the International Association for the Study of Pain {Raja et al, 2020}. In this new definition pain is described as: 'an unpleasant sensory and emotional experience associated with, or resembling that associated with, actual or potential tissue damage'. Pain is therefore not only a physical sensation, but also has its own emotional component. Although we do not yet fully understand the mechanisms of pain, we do know that there are at least three different pain pathways that connect the spinal cord with the brainstem and the brain: the ascending lateral and medial pathways and the descending inhibitory pathway.

- The lateral pathway represents the sensory component of pain and is triggered via C, Aδ, and Aβ nerve fibres. It runs through the ventral posterolateral part of the thalamus and connects with the somatosensory cortex and parietal area {Squire et al., 2008, Kulkarni et al., 2005}.
- The medial pathway represents emotional and affective pain components and is activated by C nerve fibres. It runs through the mediodorsal part of the thalamus to the anterior cingulate cortex and anterior insula {Squire et al., 2008, Kulkarni et al., 2005}.
- The descending pathway has an inhibitory effect, and thus supresses ongoing pain. It leads from the pregenual anterior cingulate cortex to the periaqueductal grey and then continues towards the peripheral nerves {Fields, 2004}. A schematic overview of the pain pathways is shown in Figure 1.

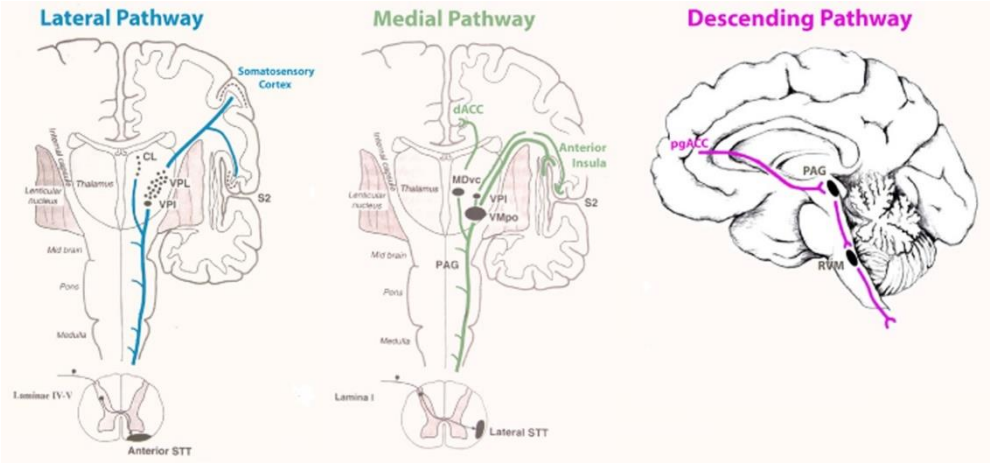

Figure 1. Schematic overview of the three pain pathways: lateral, medial and descending. Schematic from: De Ridder and Vanneste, 2016

Pain itself may be unpleasant but it is a useful warning system that protects us from getting seriously harmed. The problem is that pain loses this function when it becomes chronic, as stated by one of the pioneers of pain medicine John Bonica: 'when it becomes intractable, it no longer serves a useful purpose and then becomes, through its mental and physical effects, a destructive force' {Bonica, 1953}. Chronic pain can take over both physical and emotional aspects of a patient's life {Turk et al., 2011}. Two examples of pain syndromes causing

chronic pain are failed back surgery syndrome (FBSS) and chronic regional pain syndrome (CRPS). Patients with FBSS have persisting lower back pain after spinal surgery that sought to relieve their pain {Daniell and Osti, 2018}. CRPS usually affects one of the extremities and can develop after surgery or trauma, although its pathophysiology is still not fully understood {Maihöfner et al., 2010}. The treatment of these syndromes are preferentially physically and/or pharmaceutical but sufficient pain reduction is not achieved in all patients. A proven last resort therapy for chronic pain syndromes like FBSS and CRPS is spinal cord stimulation (SCS) {Kemler et al., 2000, Kumar et al., 2007, Sears et al., 2011}.

1.2 Spinal cord stimulation

Spinal cord stimulation was first introduced by Shealy in 1967, based on the gate control theory of Melzack and Wall. The gate control theory states that activation of the large Aβ fibres prevents pain signals, transmitted by the C and Aδ fibres, from reaching the brain by closing a hypothetical gate in the spinal cord {Melzack and Wall, 1965, Shealy et al., 1967}. A day to day example of this is pain relief that comes from rubbing a painful area. SCS achieves this same effect by electrical stimulation of the dorsal columns of the spinal cord. For SCS, electrodes are surgically placed in the epidural space, connected to a pulse generator implanted in the upper buttock. The electrodes deliver a current to the spinal cord to modulate neural bodies, axons, and synapses {Miller et al., 2016}. The most important parameters of stimulation are the pulse frequency, pulse width, amplitude, and stimulation type. The two most common stimulation types are tonic stimulation and burst stimulation.

Tonic stimulation is the conventional stimulation type. It has a fixed pulse rate, usually between 30 and 120 Hz, and causes paresthesia in the pain area {Shamji et al., 2017, Caylor et al., 2019}. Burst stimulation is a more novel variant which delivers bursts of pulses at 40 Hz, with an intraburst frequency of 500 Hz. The pulses of burst stimulation are sub-threshold, making it a paresthesia free form of SCS {De Ridder et al, 2013}.

SCS provides sufficient pain relief for two in three patients on a world wide scale, but there is no reliable metric to predict if implantation will be successful {Taylor et al., 2013}. Part of the explanation for this is that the mechanisms of action have proven to be more complex than the gate control theory alone. The complete mechanisms of action are still not fully elucidated, we do know however that the effects of SCS are not only spinal but also supraspinal {Sankarasubramanian et al., 2019, Bentley et al., 2016, Barchini et al., 2012}. Research into the supraspinal effects is based on different modalities. Functional MRI and PET scans are used to study changes in cerebral oxygenation and metabolism, but they do not measure neuronal activity directly. For this, magnetoencephalography (MEG) and electroencephalography (EEG) are the modalities of choice.

1.3 Magnetoencephalography

Synchronous activation of neurons generates electric currents and with that electric and their perpendicular magnetic fields. Where EEG detects the electric field using electrodes on the scalp, MEG detects the magnetic field with sensors placed in a helmet surrounding the head. The source of the signals detected by these modalities is the same: they detect the dendritic current of synchronised pyramidal neurons {Hämäläinen, 1991}. The measurements of the

magnetic field are in the order of femto- to pico-tesla and provide a high temporal resolution (in the order of milliseconds) of neuronal activity {Singh, 2014}.

Source estimation is a critical part of MEG measurements. It comprises a forward problem and an inverse problem. A visualisation of these problems is shown in Figure 2. Estimates for the forward and inverse problem are needed to go from the sensor space (outside of the brain) to the source space (inside the brain) and vice versa. For the forward problem a model is needed that explains how the neuronal currents produce a magnetic field, and how this radiates through the different tissues. The inverse problem presents the question how to determine active sources in the brain, from the magnetic fields detected outside of the brain. There are an infinite amount of solutions for the inverse problem, so certain assumptions have to be made in order to estimate these sources {Hämäläinen et al., 1993}.

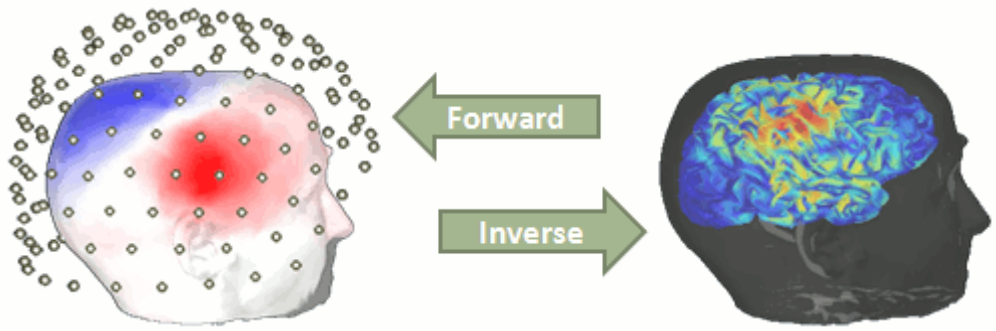

Figure 2: Visualisation of the forward and inverse problems of source estimation in MEG Image from: Brainstorm tutorial

An advantage of MEG over EEG is that the magnetic fields, unlike the electric fields, are not affected or distorted by the skull or cerebrospinal fluid. This results in MEG having a better spatial resolution for source estimation than EEG (2-3 mm for MEG compared to 7-10 mm for EEG) {Singh, 2014}. With this spatial resolution it is not only possible to detect cortical activity, but it also seems possible to detect activity of deep brain structures with MEG {Pizzo et al., 2019}.

1.4 Literature study

In my literature study I have summarised which changes in certain brain regions have been reported in EEG and MEG studies on chronic pain patients treated with continuous SCS. The period in which patients were stimulated in between MEG recordings varied from one week up to several months. Although no definitive conclusions could be drawn, two interesting trends showed up.

The first trend was that different brain regions, belonging to one of the three pain pathways, had different reactions to different types of stimulation. Most notably, structures in the medial pathway were reported to be modulated significantly more after burst stimulation compared to tonic stimulation {De Ridder et al., 2013, De Ridder and Vanneste, 2016, Lerman et al., 2019}. The cerebral structures in the medial pain pathway in which these changes due to burst SCS have been described were: the anterior insular cortex (AIC), the dorsal anterior cingulate cortex (dACC), the dorsolateral prefrontal cortex (dlPFC),

and the medial dorsal thalamus (MDT). For the lateral pathway, modulation by both tonic and burst stimulation was detected in the primary sensory cortex (S1).

Secondly, almost all studies reported modulation in the theta (4-7 Hz) and/or alpha frequency (8-12 Hz) ranges. One way of expressing changes in these bands is by determining the ratio between the power in each band. An advantage of looking at the ratios is that differences in total absolute power between patients are no longer important. These differences can be caused not only by differences in brain activity, but also, for example, by the distance between the brain and the detectors. Modulation of neuronal activity in the theta and alpha bands can signify successful SCS, although this was only reported explicitly by two studies {Schulman et al., 2005, Parker et al., 2019}. It could not be concluded from my literature study if spectral changes are related to the amount of pain reduction achieved.

These changes were all detected after stimulation of multiple days or even months. Little is known about the acute neuronal reactions to SCS and if they can even be detected. This study is therefore experimental in nature and intended to generate new hypotheses. It is therefore not expected that large significant differences will be found on a group level. If acute modulation is distinguishable, this could be very useful for determining eligibility for stimulation in general, eligibility for specific types of stimulation, and programming of the stimulation parameters.

2. Objectives

The primary objective of this TM3 study was to use MEG to analyse the acute effect of burst and tonic SCS on spectral features in the whole brain and in a subset of brain regions. The regions of interest (ROIs) are the AIC, dACC, dlPFC, thalamus, S1, and the primary visual cortex (V1). The AIC, dACC, dlPFC, and thalamus are regions that are involved in the medial pain pathway and are reported to be modulated by burst stimulation. S1 is part of the lateral pain pathway and is modulated by spinal cord stimulation in general. V1 is included as a control site; it is not part of the pain matrix, it is anatomically distanced from the other regions, and no modulation has been detected in this area {De Ridder and Vanneste, 2016}. Power spectrum densities (PSDs) were calculated to study the spectral features. A PSD allows inspection of the data in the frequency domain, it shows the power with which each frequency is present in the signal.

The secondary objective was to image changes in brain activity during the transition from ON to OFF and vice versa. For this, analysis in the time-frequency (TF) domain at the transition periods is done by computing the TF decomposition (TFD) in the 1 – 30 Hz range. It shows at which point in time the changes in the frequency domain occur. The choice for the 1 – 30 Hz frequency range is based on the results of my literature study, which has shown that changes occur primarily in the theta and alpha bands. The TFD analysis was only done for one of the patients. This patient mentioned feeling the pain increase and decrease rapidly when the stimulation was turned on or off.

The primary objective is analysed in the two following sections:

1. Analysis of the spectral effects of SCS in the whole brain sensor average
   - Comparison of stimulation ON versus stimulation OFF
   - Comparison of tonic stimulation versus burst stimulation

2. Analysis of the spectral effects of SCS in brain region source averages
   - Comparison of stimulation ON versus stimulation OFF
   - Comparison of tonic stimulation versus burst stimulation

These analyses were conducted on group level, but also on individual patients who were good responders to tonic and/or burst stimulation.

The secondary objective is analysed in one section:

3. Analyse the acute effects of SCS in the TFD
   - Analysis of the effects in the whole brain
   - Analysis of the effects in specific brain regions

The methods and results for these three steps vary, and will be discussed in separate chapters in this report (chapters 4, 5, and 6 respectively). They do however share the same data acquisition and pre-processing, which will be described in chapter 3.

3. Data acquisition and pre-processing

3.1 Patient data

The MEG data of 17 patients with chronic pain and SCS was recorded at two different locations, 9 at the Montreal Neurological Institute (MNI, Montreal, Canada) and 8 at the Donders Institute for Brain, Cognition and Behaviour (Nijmegen, the Netherlands). Table 1 provides an overview of their baseline information. In total 8 men and 9 women were included, with an average age of 56 years. The patients evaluated a week of tonic, a week of burst, and a week of placebo stimulation prior to the measurements for this study. The placebo stimulation comprised of a non-therapeutic burst stimulation variation with only two pulses per burst set to a very low amplitude possible (0.05 mA). The order of the stimulation types was randomised for each patient. After each of these weeks, the numeric rating scale (NRS) was used to score their pain, where 0 indicated no pain and 10 indicated the worst pain imaginable. The patients were asked to score their average pain of the last 24 hours of stimulation. It should be noted that some of the patients reported the lowest pain after the placebo stimulation.

Table 1: Baseline information of the included patients.

Patient	Sex	Age	NRS Tonic	NRS Burst	NRS Placebo	Localisation			Side
PT03	F	42	4	2	5	Leg			R
PT04	M	59	7	5	5	Leg	Back		L
PT05	M	52	6	7	6	Leg		Foot	R
PT06	F	45	1	2	3		Back		R, L
PT07	M	58	3	2	3	Leg	Back		L
PT08	F	42	4	2	2	Leg			L
PT09	F	62	6	9	4	Leg	Back		R
PT10	M	70	6	4	6			Foot	R, L
PT11	F	62	6	6	5	Leg	Back		R
PTN04	F	43	4	3	3	Leg	Back	Foot	L
PTN05	M	64	6	2	6		Back		R, L
PTN06	M	70	1	1	1	Leg		Foot	R
PTN07	F	56	7	7	8		Back	Foot	L
PTN08	F	40	2	5	6	Leg		Foot	R
PTN09	F	56	3	2	5	Leg	Back		R
PTN14	M	68	2	3	3	Leg	Back		R
PTN15	M	60	7	6	2	Leg	Back		L

The PT patients were recorded in Montreal and the PTN patients were recorded in Nijmegen. F: female, L: left, M: male, NRS: numeric rating scale, R: right.

3.2 Data acquisition

In both locations the patients were measured with the same 275 channel whole-head MEG system (CTF, Coquitlam) using the same acquisition software and measurement setup. The recordings took place between July 2018 and May 2019. All recordings were of resting state neuronal activity and varied in length from six to ten minutes. During the recordings the pulse generators of the patients were set to a cyclic stimulation program. In this cyclic setting the stimulation alternated between a minute of stimulation and a minute without stimulation (referred to as stimulation ON and stimulation OFF respectively). When turning on, there was a ramp of one to six seconds before the full pulse amplitude was reached, after which a full minute of stimulation started. This setting was what made it possible to study the acute effects of SCS.

The settings of the cyclic protocol were based on a trade-off between data maximisation and patient comfort. Due to their chronic pain, the patients were not able to sit still in the MEG for long periods of time. Some patients would also fall asleep during longer recordings. The one minute intervals were chosen to have a broad window to capture the acute changes, because the exact timing of when these commence is unknown (and probably varies between patients). Additionally, these intervals resemble the intervals used in fMRI studies {Moens et al., 2012}. For each patient, these recordings were done with tonic and with burst stimulation. The position of the head in the MEG was registered by marking digital head points on the head in relation to the MEG helmet.

3.3 Data pre-processing

I performed the data analysis in Brainstorm, an open-source application developed with Matlab {Tadel et al., 2011}. The following processes were used for the data cleaning: band pass filtering, notch filtering, power spectral density (PSD), artefact detection, and signal space projections (SSPs). The data was cleaned for a broader frequency range than needed for this study. This has been done deliberately in order to allow for additional research into other frequency ranges. The band pass filter was used to remove noise below 1 Hz and above 200 Hz. The low-frequency noise originates from breathing motions which can induce slow oscillations generated by metal implants. Muscle activity, for instance in the neck, can cause high-frequent noise up to 300 Hz. Muscle activity can cause noise in lower frequencies as well, but this was not filtered out by default in order to preserve the actual neuronal signals. The remaining noise was cleaned as described in the section below.

Notch filters were used to clean the data of power line contamination by applying filters at the power line's frequency and higher harmonics up to 200 Hz. The power line frequency is country dependent, 50 Hz for the Netherlands (the Donders Institute) and 60 Hz for Canada (the MNI). In some patients the SCS itself also contaminates the recordings. For these individual cases, additional notch filters were used to remove the stimulation frequency and its higher harmonics from the data. These extra artefacts were clearly visible in the PSD. The PSDs were calculated with the Welch method, using a window of four seconds with 50% overlap.

Artefacts from heartbeats and eye movement (blinking and saccades) were present in all recordings. To detect these artefacts, the Brainstorm function used the electrocardiogram (ECG) for heartbeats, and the vertical electrooculogram (EOG) data for blinks and the horizontal EOG for saccades. Automatic detection of 40-200 Hz activity was used to find remaining muscle activity artefacts. These events were then also marked in the raw signal. Events that occur in a similar fashion in a similar location (like heartbeats and blinks) will cause a similar response in the sensors. SSPs were computed using principle components analysis (PCA) to remove the artefacts from the data {Tesche et al., 1995, Uusitalo et al., 1997}. Which component was used to create an SSP was based on the topology of each component. For example, blinks are evidently picked up by frontal sensors while activity in the neck muscles shows up as a semi-circle at the occipital sensors. An example of a blink SSP is shown in Figure 3.

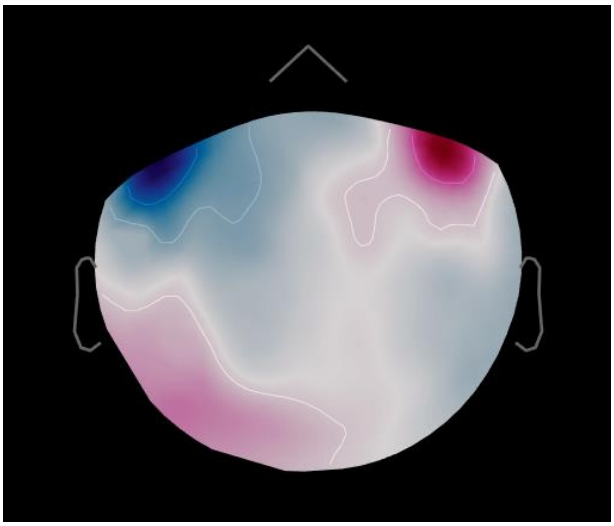

Figure 3: Example of a signal space projection used to remove blink artefacts from the data.

4. Sensor space analysis

In this chapter the average effect of SCS on the whole brain is described. The analyses were done at the sensor level by using the average of all sensors. This chapter is divided in a methods section, and three results sections: stimulation ON versus stimulation OFF, tonic stimulation versus burst stimulation, and responses of individual patients.

4.1 Methods

The first step in the analysis was to separate the segments with and without stimulation from the continuous MEG signal. These segments were determined by using the stimulation artefact in the ECG recording. For each recording I determined the beginning of the first full cycle, and marked when the stimulation was on or off. In three of the twenty patients it was not possible to determine the cycles, because stimulation artefacts were not detectable. These three patients were excluded from further analysis. The recordings of the remaining seventeen patients were imported in Matlab and automatically split, based on the starting time of the first cycle and the duration of the ramp. The ramp sections were cut out, resulting in segments of 60 seconds of stimulation and 60 seconds without stimulation. If the segment before the first full cycle was longer than 45 seconds, it was also included.

From these segments, the PSD with stimulation ON and the PSD with stimulation OFF were computed using the Welch method with a window of four seconds and 50% overlap. These PSDs were then normalised by dividing the power in each frequency bin by the sum of the power in the range from 1 to 62 Hz. The upper limit of 62 Hz was chosen to make sure that the notched power line frequency (either at 50 or 60 Hz) would always be included. It was not set at a lower frequency to allow for inspection of other frequency ranges in possible future research.

From these PDSs, three ratios were calculated which all describe different modulations of theta and alpha frequency power. The sum of the power was calculated for each frequency range and these were then divided by each other for each individual patient. These ratios were based on the results from my literature study, mainly on the work of Schulman et al., De Ridder et al., and Telkes et al. {Schulman et al., 2005, De Ridder et al., 2013, Telkes et al., 2020}. The three ratios were:

- Ratio 1: high-theta to low-alpha (7-9/9-11 Hz) {Schulman et al., 2005}
- Ratio 2: theta to alpha (4-7/7-12 Hz) {Telkes et al., 2020}
- Ratio 3: low-alpha to high-alpha (8-10/10-12 Hz). {De Ridder et al., 2013, Telkes et al., 2020}

Paired two-tailed t-tests were performed to determine the significance of group level differences. Correction for multiple testing was not performed, as the intention of this study was to identify directions for future research, not to identify irrefutable differences. The individual PSDs were averaged and plotted as one PSD.

Patients were included for the individual analysis if their pain score was decreased by more than 50% after the week of tonic or burst stimulation compared to the placebo week.

4.2 Results: stimulation ON versus stimulation OFF

The results of the sensor-average comparison between stimulation ON and stimulation OFF are shown in Table 2, the corresponding PSDs are shown in Figures 4a-d. Ratio 1 increased in the ON state, independent of stimulation type and normalisation. This indicates that generally when the stimulation is ON, there was relatively more power in the 7-9 Hz and less power in de 9-11 Hz band than when the stimulation was OFF. Although the differences were not significant, the effect size was the largest for Ratio 1, with an average increase of 2.5% in the ON state. Ratio 2 decreased by 1.5% during stimulation ON in all categories. It also showed the lowest p-values of the three ratios. Ratio 3 showed the smallest effect size, on average a 0.5% increase during stimulation ON. It also has the highest p-values, this indicates that the power in these two frequency bands does not change during the cyclic stimulation.

Table 2: Stimulation ON versus stimulation OFF, overview of average frequency ratios and the p-values of the difference between stimulation ON and stimulation OFF for tonic and burst stimulation.

		Ratio 1 high theta/low alpha [7-9/9-11 Hz]		Ratio 2 theta/alpha [4-7/7-12 Hz]		Ratio 3 low alpha/high alpha [8-10/10-12 Hz]	
		ON	OFF	ON	OFF	ON	OFF
Average	Both absolute	1.20	1.17	0.67	0.68	1.72	1.71
Average	Both relative	1.19	1.16	0.73	0.74	1.63	1.62
Average	Burst absolute	1.17	1.15	0.67	0.68	1.73	1.71
Average	Tonic absolute	1.23	1.20	0.67	0.68	1.71	1.71
Average	Burst relative	1.18	1.15	0.74	0.75	1.63	1.62
Average	Tonic relative	1.21	1.18	0.72	0.73	1.63	1.62
P-value	Both absolute	0.18		0.13		0.82	
P-value	Both relative	0.16		0.02		0.60	
P-value	Burst absolute	0.43		0.10		0.69	
P-value	Tonic absolute	0.26		0.43		0.89	
P-value	Burst relative	0.35		0.03		0.67	
P-value	Tonic relative	0.33		0.15		0.76	

In this table "both" refers to the combination of the tonic and burst stimulation data.

In the PSDs of the sensor space analyses, a marginal increase in power is visible around 9 Hz in the stimulation ON plot compared to stimulation OFF (Figure 4). The standard errors almost completely overlap, indicating that the PSDs are not significantly different.

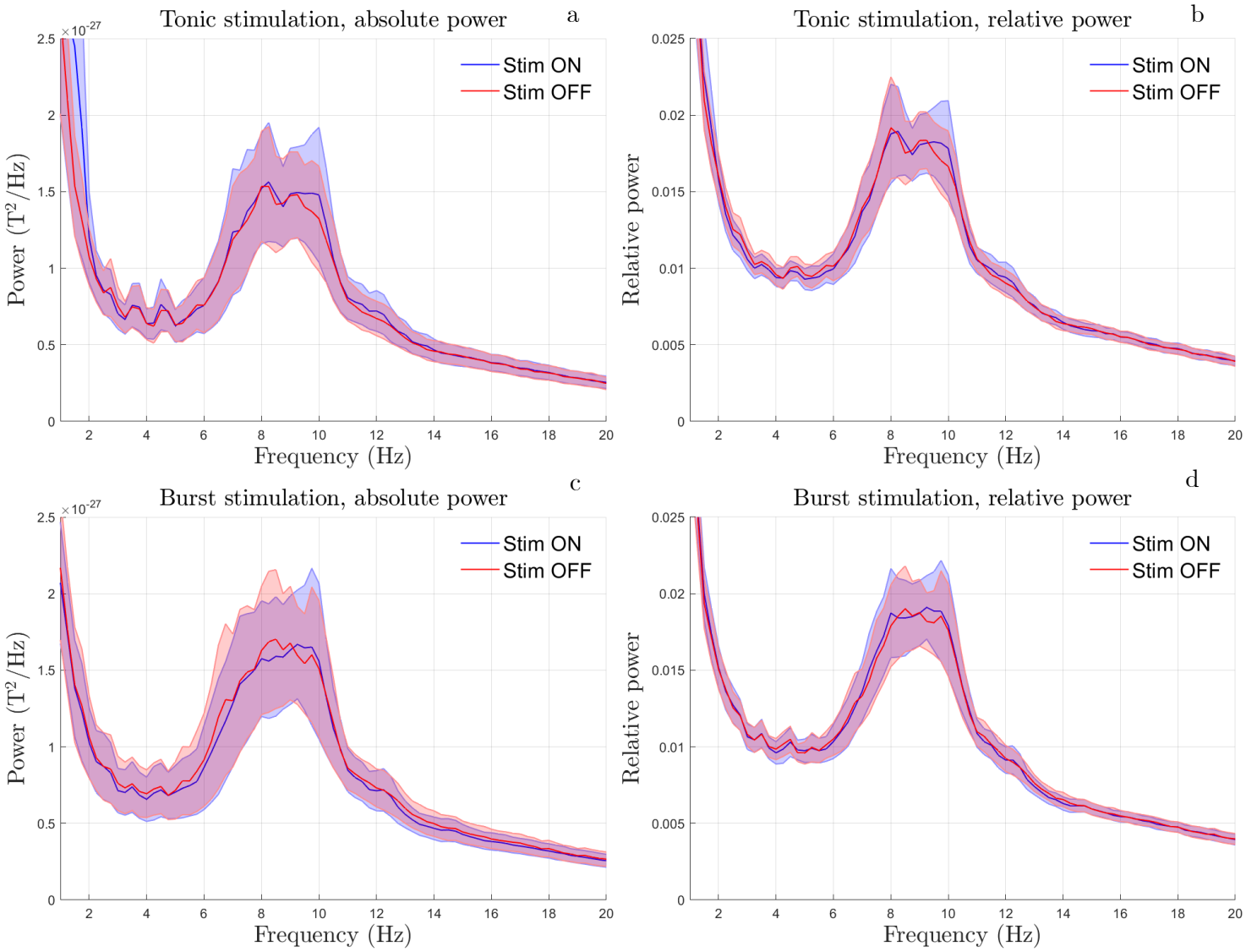

Figure 4 a-d: The average PSDs with standard error (shaded) for all 17 patients, comparing stimulation ON (blue) vs. OFF (red). (a) shows absolute power for tonic stimulation, (b) shows relative power for tonic stimulation, (c) shows absolute power for burst stimulation, (d) shows relative power for burst stimulation.

4.3 Results: tonic stimulation versus burst stimulation

The results of the sensor-average comparison between tonic and burst stimulation are shown in Table 3. The corresponding PSDs are shown in Figures 5a-d. During tonic stimulation, Ratio 1 increased by 3.5% compared to burst stimulation, both during the ON state and during the OFF state. This means that there was more power in the 9-11 Hz band during burst stimulation, both during stimulation ON and OFF. Ratio 2 was equal for the absolute data but tonic decreased by 2.5% compared to burst stimulation in the relative data. Ratio 3 only differs in absolute ON, where it is slightly decreased during tonic stimulation. The effect size was largest for Ratio 1, which also showed the lowest p-values.

Table 3: Tonic stimulation versus burst stimulation, overview of the average frequency ratios and the p-values of the difference between stimulation ON and the differences between stimulation OFF.

		Ratio 1 high theta/low alpha [7-9/9-11 Hz]		Ratio 2 theta/alpha [4-7/7-12 Hz]		Ratio 3 low alpha/high alpha [8-10/10-12 Hz]	
		Tonic	Burst	Tonic	Burst	Tonic	Burst
Average	ON absolute	1.23	1.17	0.67	0.67	1.71	1.73
Average	OFF absolute	1.20	1.15	0.68	0.68	1.71	1.71
Average	ON relative	1.21	1.18	0.72	0.74	1.63	1.63
Average	OFF relative	1.18	1.15	0.73	0.75	1.62	1.62
P-value	ON absolute	0.26		1.00		0.68	
P-value	OFF absolute	0.36		0.96		0.98	
P-value	ON relative	0.45		0.26		0.96	
P-value	OFF relative	0.47		0.32		0.89	

Figures 5a and 5b show that the average absolute power in the range of 4 – 12 Hz is higher during burst stimulation compared to tonic stimulation. This difference decreases after normalisation, but Figures 5c and 5d still show a marginal increase during burst stimulation, mainly in the 9 – 10 Hz range.

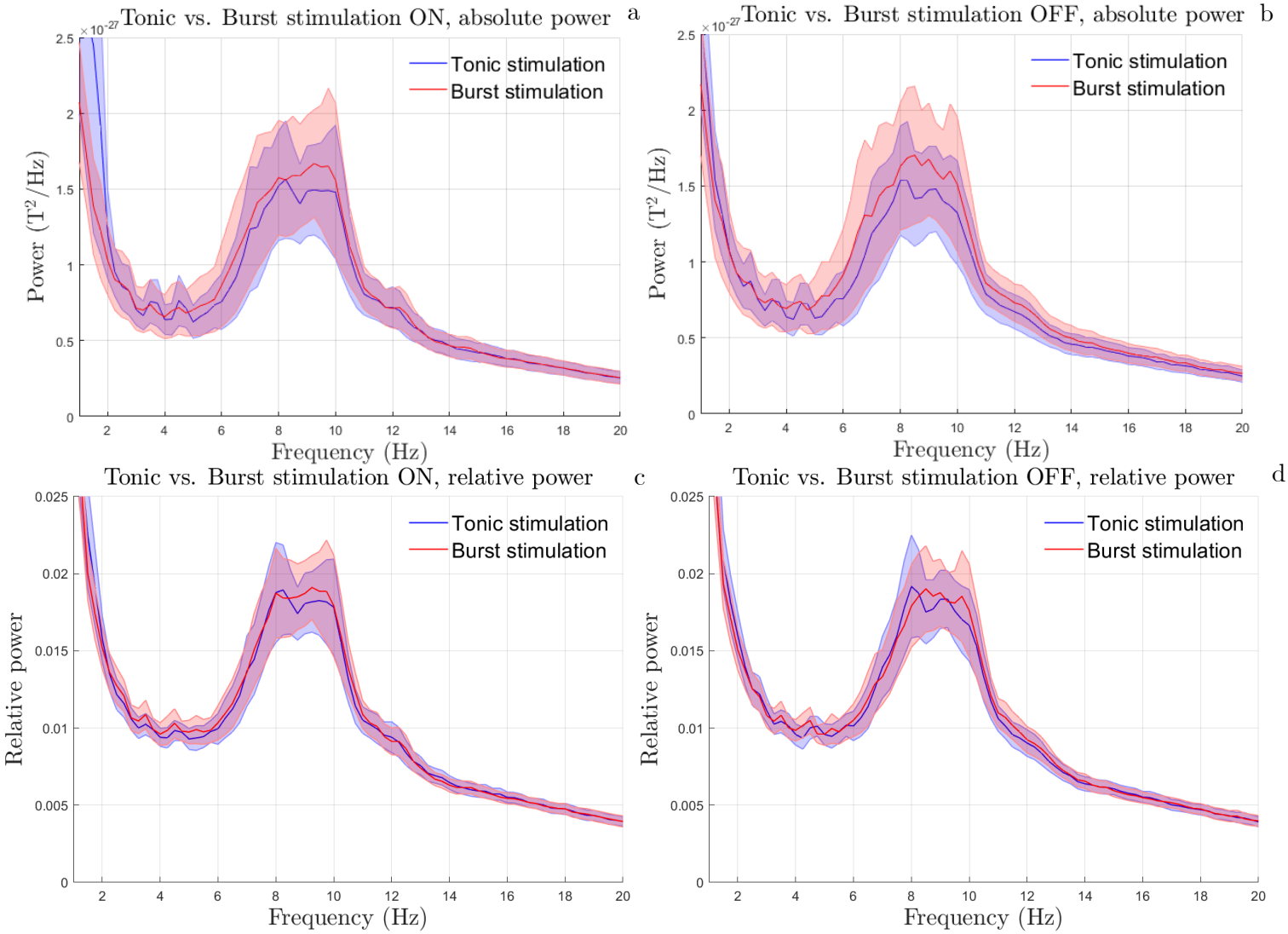

Figure 5 a-d: The average PSDs with standard error (shaded) for all 17 patients, comparing tonic stimulation (blue) vs. burst stimulation (red). (a) shows absolute power for stimulation ON, (b) shows relative power for stimulation OFF, (c) shows absolute power for stimulation ON, (d) shows relative power for stimulation OFF.

4.4 Results: individual patients

The pain score decreased by 50% or more for two patients after the week of burst stimulation (PT03 and PTN05) and for one patient after the week of tonic stimulation (PTN08). I also chose to include PT06 because she indicated feeling her pain wax and wane during the cyclic stimulation. Although these patients were all good responders to SCS, their individual results varied.

The four panels in Figure 6 show the PSDs for stimulation ON (red) versus OFF (blue) for the four individual patients. Panels 6a and 6b show the PSDs for burst stimulation for PT03 and PTN05, respectively. PSDs of tonic stimulation ON versus OFF were shown in panels 6c and 6d for PT06 and PTN08. The individual PSDs and the differences between ON and OFF were all different when comparing the four patients. PT03 shows a sharp increase in power at 7 and 9 Hz during stimulation ON, while PTN05 shows a broad increase in power between 8-10 Hz during stimulation ON. PT06 barely showed any change, and PTN08 showed increased power at 9 and 10 Hz.

A commonality between PT03, PTN05, and PTN08 is that the power increased when the stimulation was ON. The variation displayed here was exemplary for all other comparisons, which can be seen in Appendix 10.1.

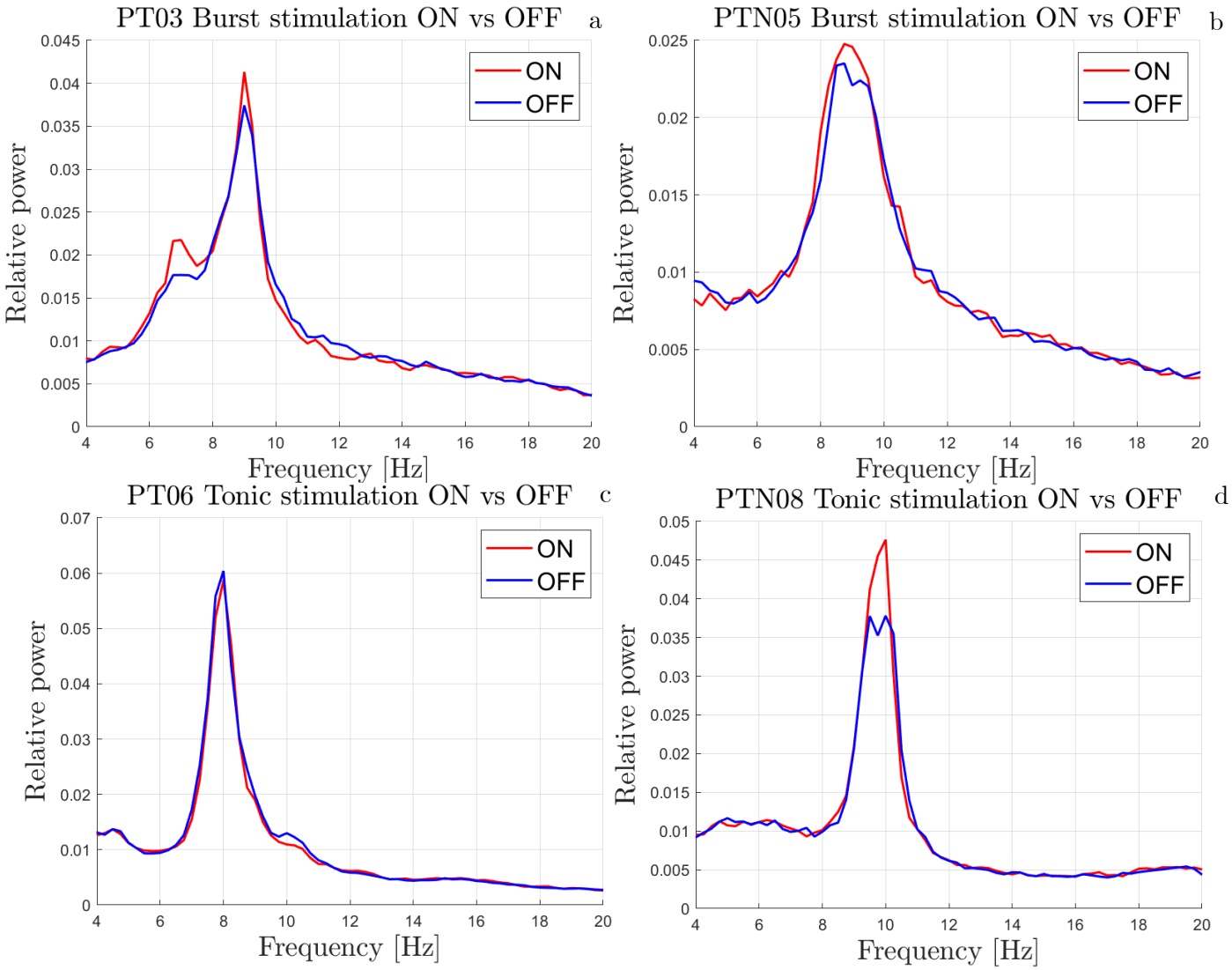

Figure 6 a-d: The four individual PSDs, comparing stimulation ON (red) vs. OFF (blue). (a) shows PT03 for burst stimulation, (b) shows PTN05 for burst stimulation, (c) shows PT06 for tonic stimulation, (d) shows PTN08 for tonic stimulation.

5. Source space analysis

In this chapter the neuronal activity is analysed in more detail. By estimating the sources of the activity it is possible to analyse modulation of neuronal activity in specific brain regions. This chapter contains four sections: methods, and results of stimulation ON versus OFF, tonic stimulation versus burst stimulation, and the response of the individual patients.

5.1 Methods

The SCS systems of the patients were not compatible with MRI, therefore the default ICBM152 MRI anatomy, available in Brainstorm, was used for each patient. The positions of the registered head points were checked before the data cleaning. The default anatomy was then warped to fit these head points. Six fiducial points were marked in the MRI volume: the nasion, left and right pre-auricular points, the anterior and posterior commissure, and an interhemispheric point. With these points the MRI was fitted to the digitised head points. To compute group statistics, a common reference frame was needed for the head models. This was created by computing the MNI transformation for each MRI volume {Ashburner et al., 2005}. The MNI space stores a normalised transformation of the warped MRI that allows referencing with other MRI volumes.

To compare the source estimations of the different patients a shared grid was projected on the MNI subject space. Using this template grid, the sources of neuronal activity were estimated, and thereby a solution for the inverse problem was approximated. A regular isotropic grid was generated, consisting of 13381 grid points equally distributed across the entire brain. These grid points represented the amount of dipoles that were estimated in the source localisation. A new MRI volume head model was then generated for each patient based on the new template grid.

Various solutions exist to estimate the activity in the thousands of grid points based on the measurements of a few hundred sensors, the most common of which are implemented in Brainstorm. Three different settings needed to be determined: the computation method, the normalisation method, and the dipole orientations. The recommended setting for sources that are expected to be distributed is minimum norm imaging, as it is the least restrictive in source assumptions. This method favours the minimum energy solutions, while also suppressing noise based on the noise covariance {Hämälainen et al., 1994}. The noise covariance was calculated from empty room noise recordings taken at the start of each recording day. The noise recordings were pre-processed with the same notch and frequency filters as the patient recordings. The result of the minimum norm estimate is a linear kernel that can be multiplied with the spatial data to acquire the current in each point in the source grid.

The measure for this current density could be normalised to increase the values of deeper areas. This is however not recommended for averaging across MEG runs or time-frequency decompositions, so I chose not to perform any normalisation on the source model.

For the dipole orientation, I used an unconstrained approach. At each grid point, a current dipole can be aiming along one of the three axes, but this orientation can also be constrained. When working with surface grids for cortex models the dipole orientation is constrained.

Here, only one dipole is modelled at each grid point, with its orientation perpendicular to the cortex. This is done because the pyramidal neurons are in columns oriented perpendicular to the cortical surface. When working with volume models this simplification is not accurate anymore because we are now also interested in activity from deeper regions. In those cases, the use of an unconstrained approach is advised by the Brainstorm team. Now, at each grid point three dipoles are defined, with orientations perpendicular to the three axes. This enables the combined current to point in any direction.

We now have a model with the neuronal activity at each grid point but are interested in the activity in certain regions comprising multiple grid points. Therefore, the grid points were grouped with the automated anatomical labelling (AAL) atlas which is freely available online {Tzourio-Mazoyer et al., 2002}. Both cortical and deep structures are included in this segmentation, as can be seen in Figure 7. The image on the left is the full AAL atlas, and the image on the right are the ROIs: the dlPFC (burgundy), dACC (orange), Insula (red), S1 (blue), V1 (magenta) and thalamus (not visible in this image).

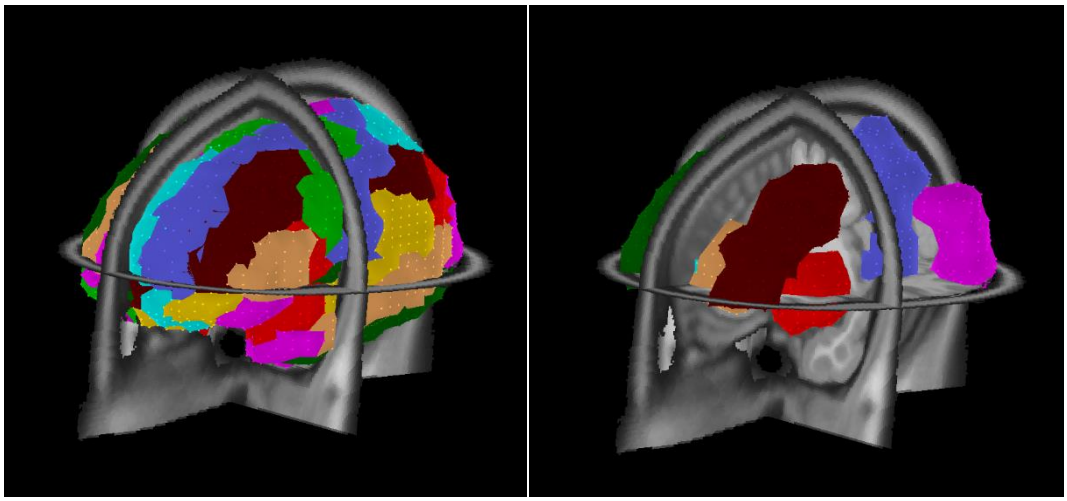

Figure 7: 3D MRI view of the complete AAL volume atlas on the left, and on the right the ROIs in this atlas; dlPFC (burgundy), dACC (orange), Insula (red), S1 (blue), V1 (magenta) and thalamus (not visible in this image).

After implementing this atlas, the average activity of the grid points in each region was estimated. The data of each of the regions was then again split in segments with and without stimulation and PSDs were calculated and normalised. Brainstorm computes the norm of the vectorial sum of the three orientations at each grid point for the normalisation. The lower limit for the normalisation was set to 4 Hz instead of 1 Hz. This was done because there was a large variation in remaining low frequent noise between the ROIs. Only the normalised values were compared due to the large differences in absolute power between the patients.

5.2 Results: stimulation ON versus stimulation OFF

Table 4 shows an overview of the differences in ratios between tonic stimulation ON and OFF in the selected brain regions. The changes in the right dlPFC are (borderline) significant, showing a decreased Ratio 2 and an increased Ratio 3 when tonic stimulation is ON. The right sensory cortex also showed a decrease in Ratio 2. The right primary visual cortex shows an increase in Ratio 1 during tonic stimulation. The effect size was largest for Ratio 2.

Table 4: Tonic stimulation ON versus tonic stimulation OFF, overview of the average frequency ratios and the p-values of the difference between stimulation ON and stimulation OFF per region.

	Ratio 1 theta/alpha [7-9/9-11 Hz]		Ratio 2 theta/alpha [4-7/7-12 Hz]		Ratio 3 alpha/alpha [8-10/10-12 Hz]	
	ON	OFF	ON	OFF	ON	OFF
dlPFC R Tonic	1.15	1.16	1.26	1.30	1.21	1.17
P-value	0.57		0.07		0.05	
dlPFC L Tonic	1.31	1.26	2.95	3.23	1.30	1.28
P-value	0.49		0.29		0.39	
V1 R Tonic	1.17	1.12	0.62	0.63	1.75	1.73
P-value	0.12		0.45		0.46	
V1 L Tonic	1.08	1.06	0.71	0.73	1.54	1.57
P-value	0.31		0.35		0.50	
Thalamus R Tonic	1.55	1.56	1.58	1.48	1.79	1.76
P-value	0.96		0.37		0.25	
Thalamus L Tonic	1.44	1.42	2.06	1.98	1.66	1.67
P-value	0.68		0.36		0.79	
S1 R Tonic	1.11	1.06	0.76	0.79	1.32	1.30
P-value	0.26		0.07		0.57	
S1 L Tonic	1.07	1.06	0.83	0.83	1.42	1.38
P-value	0.61		0.91		0.43	
Insula R Tonic	1.57	1.61	1.06	1.06	1.78	1.76
P-value	0.38		0.93		0.77	
Insula L Tonic	1.56	1.52	2.31	2.29	1.83	1.87
P-value	0.57		0.60		0.45	
dACC R Tonic	1.45	1.42	2.63	2.80	1.48	1.46
P-value	0.68		0.23		0.32	
dACC L Tonic	1.51	1.45	3.00	3.38	1.54	1.52
P-value	0.54		0.29		0.42	

dlPFC: dorsolateral prefrontal cortex, V1: primary visual cortex, S1: primary sensory cortex, dACC: dorsal anterior cingulate cortex, R: right, L: left

Table 5 provides an overview of the differences between burst stimulation ON and OFF. Most notable were the increases in the left and right S1 in all ratios. Ratio 2 slightly decreased during the ON state in the dlPFC, thalamus, and dACC.

Table 5: Burst stimulation ON versus burst stimulation OFF, overview of average frequency ratios and the p-values of the difference between stimulation ON and stimulation OFF per region.

	Ratio 1 high theta/low alpha [7-9/9-11 Hz]		Ratio 2 theta/alpha [4-7/7-12 Hz]		Ratio 3 Low alpha/high alpha [8-10/10-12 Hz]	
	ON	OFF	ON	OFF	ON	OFF
dlPFC R Burst	1.10	1.09	1.18	1.14	1.16	1.15
P-value	0.63		0.26		0.50	
dlPFC L Burst	1.14	1.11	1.49	1.53	1.20	1.16
P-value	0.14		0.49		0.07	
V1 R Burst	1.18	1.18	0.66	0.65	1.82	1.82
P-value	1.00		0.67		0.95	
V1 L Burst	1.08	1.07	0.71	0.69	1.57	1.56
P-value	0.85		0.54		0.81	
Thalamus R Burst	1.53	1.53	1.05	1.09	1.68	1.67
P-value	1.00		0.62		0.87	
Thalamus L Burst	1.38	1.38	1.27	1.33	1.59	1.60
P-value	0.96		0.42		0.94	
S1 R Burst	1.08	1.01	0.75	0.70	1.40	1.31
P-value	0.03		0.31		0.03	
S1 L Burst	1.06	1.01	0.77	0.74	1.39	1.33
P-value	0.10		0.45		0.16	
Insula R Burst	1.55	1.57	1.04	1.01	1.78	1.76
P-value	0.71		0.63		0.66	
Insula L Burst	1.51	1.48	1.21	1.20	1.79	1.79
P-value	0.41		0.66		0.92	
dACC R Burst	1.35	1.36	1.53	1.54	1.39	1.37
P-value	0.73		0.88		0.21	
dACC L Burst	1.37	1.38	1.70	1.75	1.44	1.41
P-value	0.74		0.52		0.07	

dlPFC: dorsolateral prefrontal cortex, V1: primary visual cortex, S1: primary sensory cortex, dACC: dorsal anterior cingulate cortex, R: right, L: left

5.3 Results: tonic stimulation versus burst stimulation

Table 6 shows an overview of the differences in ratios between tonic and burst stimulation in the ON state. The dlPFC and dACC showed the largest effect size in Ratio 1, with a lower ratio during burst stimulation. Ratio 2 showed the largest differences between tonic and burst stimulation. Especially the (left) dlPFC, thalamus, left insula, and the dACC clearly showed a lower Ratio 2 for burst stimulation ON compared to tonic stimulation ON. This same pattern is visible for Ratio 3, although less prominent.

Table 6: Tonic stimulation versus burst stimulation, overview of the average frequency ratios and the p-values of the difference between stimulation ON and the differences between stimulation OFF per region.

	Ratio 1 high theta/low alpha [7-9/9-11 Hz]		Ratio 2 theta/alpha [4-7/7-12 Hz]		Ratio 3 Low alpha/high alpha [8-10/10-12 Hz]	
	Tonic	Burst	Tonic	Burst	Tonic	Burst
dlPFC R ON	1.15	1.10	1.26	1.18	1.21	1.16
P-value	0.10		0.42		0.06	
dlPFC L ON	1.31	1.14	2.95	1.49	1.30	1.20
P-value	0.21		0.33		0.32	
V1 R ON	1.17	1.18	0.62	0.66	1.75	1.82
P-value	0.92		0.22		0.41	
V1 L ON	1.08	1.08	0.71	0.71	1.54	1.57
P-value	0.98		0.94		0.39	
Thalamus R ON	1.55	1.53	1.58	1.05	1.79	1.68
P-value	0.68		0.35		0.13	
Thalamus L ON	1.44	1.38	2.06	1.27	1.66	1.59
P-value	0.25		0.34		0.20	
S1 R ON	1.11	1.08	0.76	0.75	1.32	1.40
P-value	0.59		0.83		0.13	
S1 L ON	1.07	1.06	0.83	0.77	1.42	1.39
P-value	0.78		0.46		0.72	
Insula R ON	1.57	1.55	1.06	1.04	1.78	1.78
P-value	0.72		0.74		0.88	
Insula L ON	1.56	1.51	2.31	1.21	1.83	1.79
P-value	0.53		0.33		0.37	
dACC R ON	1.45	1.35	2.63	1.53	1.48	1.39
P-value	0.26		0.36		0.14	
dACC L ON	1.51	1.37	3.00	1.70	1.54	1.44
P-value	0.24		0.35		0.15	

dlPFC: dorsolateral prefrontal cortex, V1: primary visual cortex, S1: primary sensory cortex, dACC: dorsal anterior cingulate cortex, R: right, L: left

In Table 7 an overview is given of the differences in ratios between tonic and burst stimulation in the OFF state. In the OFF state, a similar pattern is visible as in the ON state: lower ratios for the burst states. Again these differences are the most prominent in the dlPFC, thalamus, Insula, and dACC.

Table 7: Overview of average frequency ratios and the p-values of the difference between tonic stimulation off and burst stimulation off per region.

	Ratio 1 high theta/low alpha [7-9/9-11 Hz]		Ratio 2 theta/alpha [4-7/7-12 Hz]		Ratio 3 Low alpha/high alpha [8-10/10-12 Hz]	
	Tonic	Burst	Tonic	Burst	Tonic	Burst
dlPFC R OFF	1.16	1.09	1.30	1.14	1.17	1.15
P-value	0.04		0.09		0.49	
dlPFC L OFF	1.26	1.11	3.23	1.53	1.28	1.16
P-value	0.04		0.32		0.13	
V1 R OFF	1.12	1.18	0.63	0.65	1.73	1.82
P-value	0.22		0.47		0.42	
V1 L OFF	1.06	1.07	0.73	0.69	1.57	1.56
P-value	0.83		0.27		0.82	
Thalamus R OFF	1.56	1.53	1.48	1.09	1.76	1.67
P-value	0.31		0.31		0.22	
Thalamus L OFF	1.42	1.38	1.98	1.33	1.67	1.60
P-value	0.30		0.34		0.21	
S1 R OFF	1.06	1.01	0.79	0.70	1.30	1.31
P-value	0.26		0.10		0.87	
S1 L OFF	1.06	1.01	0.83	0.74	1.38	1.33
P-value	0.13		0.12		0.24	
Insula R OFF	1.61	1.57	1.06	1.01	1.76	1.76
P-value	0.34		0.11		0.96	
Insula L OFF	1.52	1.48	2.29	1.20	1.87	1.79
P-value	0.18		0.32		0.13	
dACC R OFF	1.42	1.36	2.80	1.54	1.46	1.37
P-value	0.12		0.33		0.06	
dACC L OFF	1.45	1.38	3.38	1.75	1.52	1.41
P-value	0.10		0.33		0.07	

dlPFC: dorsolateral prefrontal cortex, V1: primary visual cortex, S1: primary sensory cortex, dACC: dorsal anterior cingulate cortex, R: right, L: left

6. Time frequency decomposition

The secondary objective was to image the changes in brain activity during the transition from ON to OFF and vice versa. For this, analysis in the TF domain of segments at the transition points was done by computing the TFD for PT06. I chose PT06 for these analyses because she was the only patient of whom we knew that her pain sensation changed during the cyclic stimulation. The heterogeneity of the results from the individual PSDs in chapter 4 supports the choice to analyse the spectral modulation on an individual level.

6.1 Methods

Ideally, the TFD of the entire MEG time series would be computed at once, but due to computational limits that was not possible. Therefore time segments around the transitions were used. The segments started ten seconds plus the ramp time before the transition, and ended twenty seconds after the transition in stimulation. For tonic stimulation, six transitions from both OFF to ON and ON to OFF were included. The burst stimulation had seven transitions from OFF to ON, and six from ON to OFF.

The TFD was calculated by convolution of the signal with a series of complex Morlet wavelets {Bruns, 2004}. The wavelets are shaped like a sinusoid but weighted by a Gaussian kernel, this allows them to capture local oscillatory components in the time series. The wavelets can be tuned to change the temporal and spectral resolution of the TFD. These two resolutions act as communicating vessels: when one is increased, the other is decreased. The tuning is done by changing the central frequency and time resolution of the wavelet. I used the default wavelet with a central frequency of 1 Hz and a time resolution of 3 seconds.

The TFD was computed in the 1 – 30 Hz range with steps of 0.5 Hz. For each segment this computation was first done for each sensor, after which these TFDs were averaged to generate one sensor-average TFD per segment. These were then again averaged to obtain one TFD for the transition from OFF to ON, and one TFD for the transition from ON to OFF. Secondly, the TFDs were computed for each scout, and again averages for the two transitions were calculated. Z-score normalisations were then computed for each TFD to determine and visualise the statistical differences. The first ten seconds of each segment were used as baseline.

In chapters 4 and 5 the most notable differences were seen in Ratio 2 (4-7/7-12 Hz). Therefore the average power in the 7-12 Hz band per time point was also computed from the TFDs to visualise the power change in this band over time. The average power during stimulation ON, OFF, and the ramp were then computed from the averages per time point.

6.2 Results: sensor space

The average TFD for the transition from tonic stimulation OFF to ON is shown in Figure 8. A brief drop in power in the alpha band is visible at 13 seconds, when the stimulation reaches its full power. The average TFD for the transition from tonic stimulation ON to OFF is shown in Figure 9. No clear changes in power were visible after the stimulation is turned off.

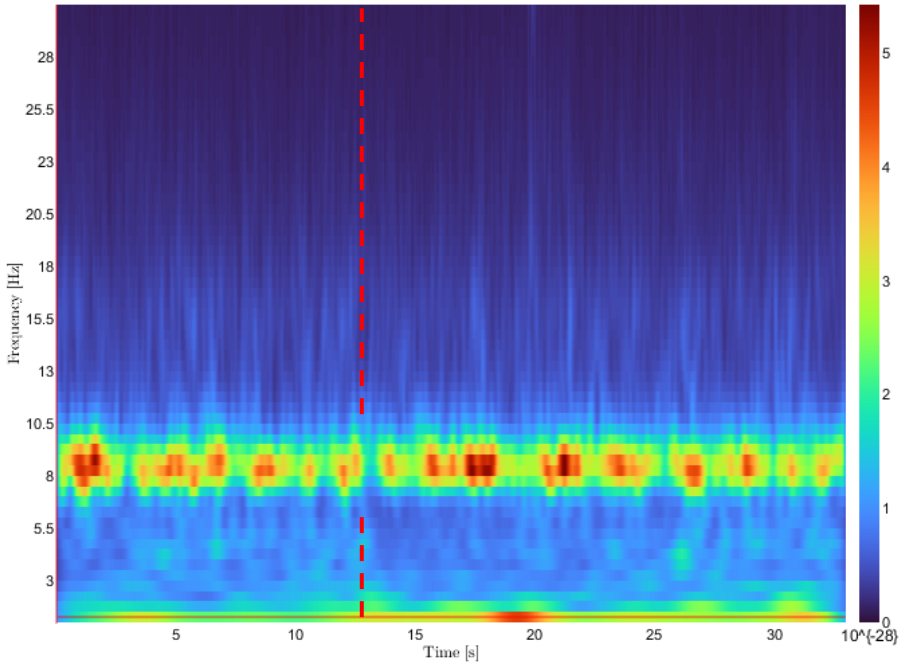

Figure 8: Transition from tonic stimulation OFF to ON in PT06: time frequency decomposition. The ramp starts at 10 seconds and the full stimulation starts at 13 seconds (dashed red line).

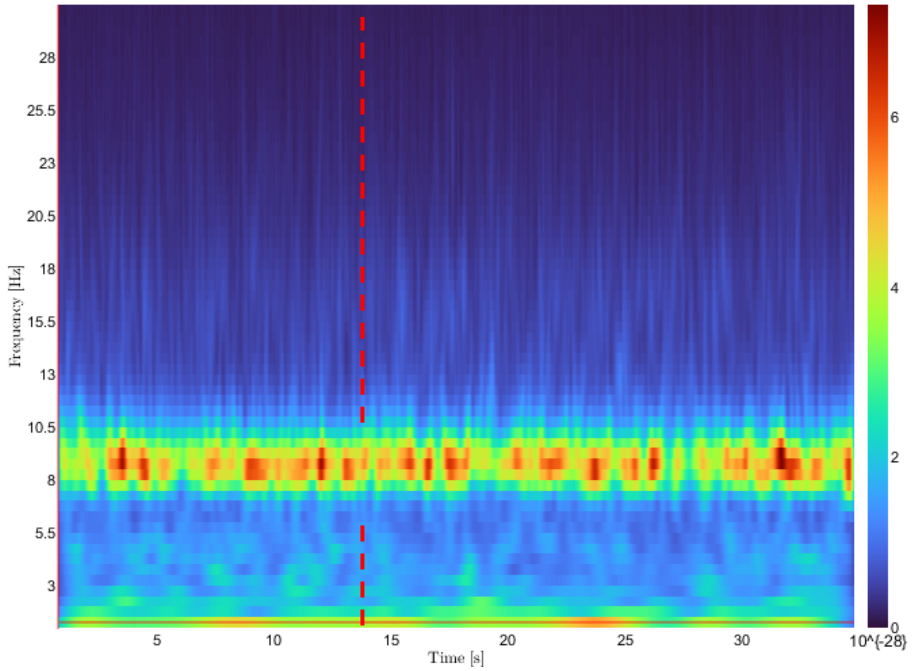

Figure 9: Transition from tonic stimulation ON to OFF in PT06: time frequency decomposition. The stimulation stops at 13 seconds (dashed red line).

The Z-score normalisation of the transition from tonic stimulation OFF to ON is shown in Figure 10. The power drop in the alpha band at 13 seconds shows a Z score of -3. The theta band also has a negative Z score for a few seconds after the stimulation turns ON.

The Z scores of the transition from tonic stimulation ON to OFF are shown in Figure 11. A sudden drop in the alpha band is visible just as the stimulation changes at 13 seconds.

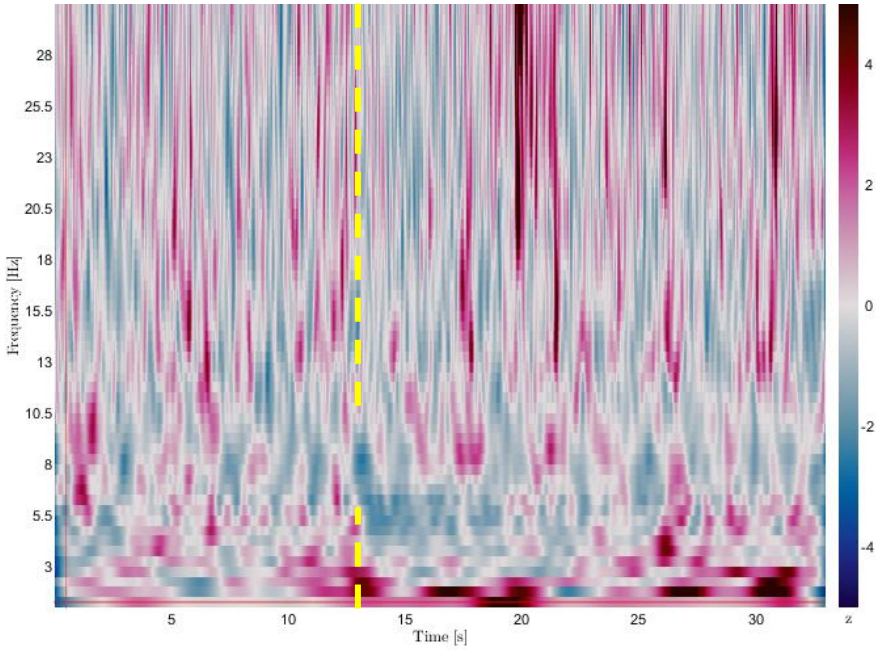

Figure 10: Transition from tonic stimulation OFF to ON in PT06: Z-scores of the time frequency decomposition. The ramp starts at 10 seconds and the full stimulation starts at 13 seconds (dashed yellow line).

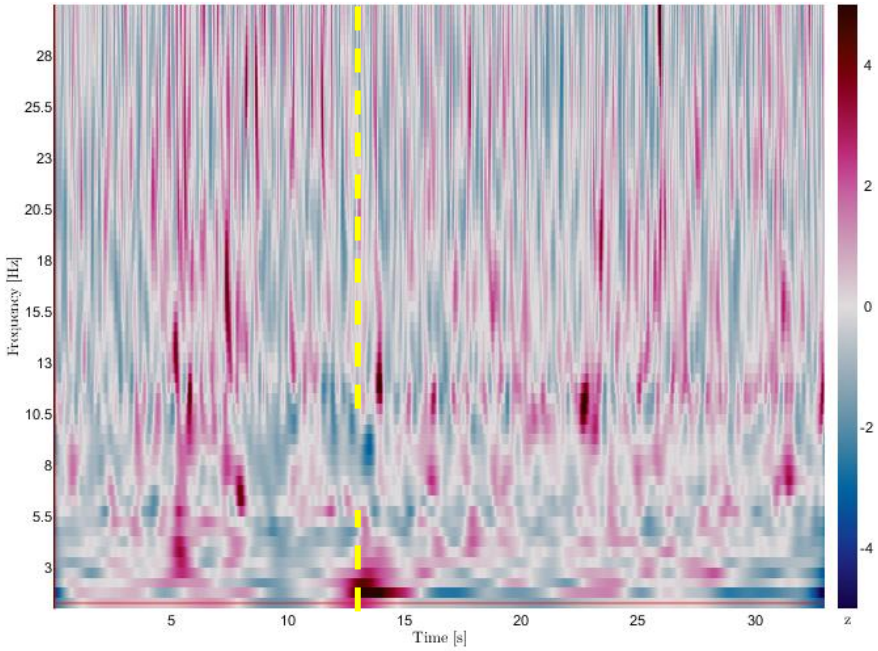

Figure 11: Transition from tonic stimulation ON to OFF in PT06: Z-scores of the time frequency decomposition. The stimulation stops at 13 seconds (dashed yellow line).

In Figures 12 and 13 the average alpha power per time point and the average power during stimulation ON, OFF, and the ramp are shown for the transitions during tonic stimulation. Figure 12 shows the transition from OFF to ON. A decrease in power was visible during the ramp and briefly after the stimulation was fully ON. Figure 13 shows the transition from ON to OFF. A sharp decrease in power was visible when the stimulation turned OFF. The average power was lower when the stimulation was ON compared to OFF.

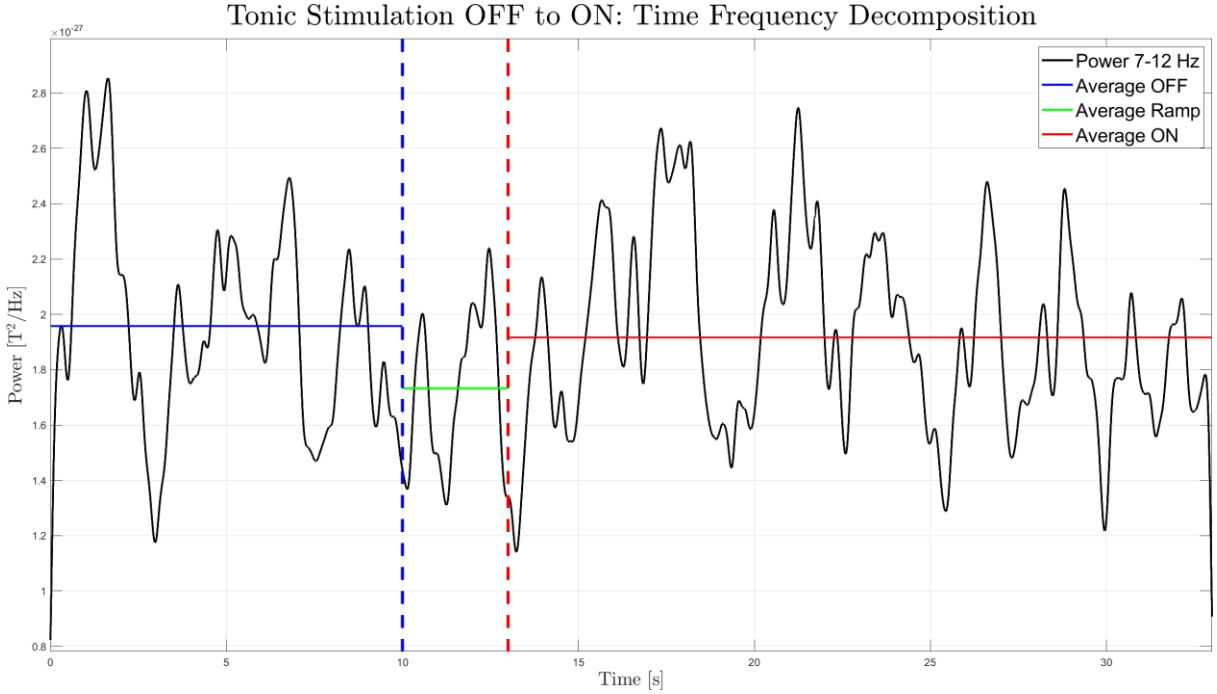

Figure 12: Average power of the 7 – 12 Hz band per time point in the TFD (black), average power during tonic stimulation OFF (blue) and ON (red), and the average power during the ramp (green).

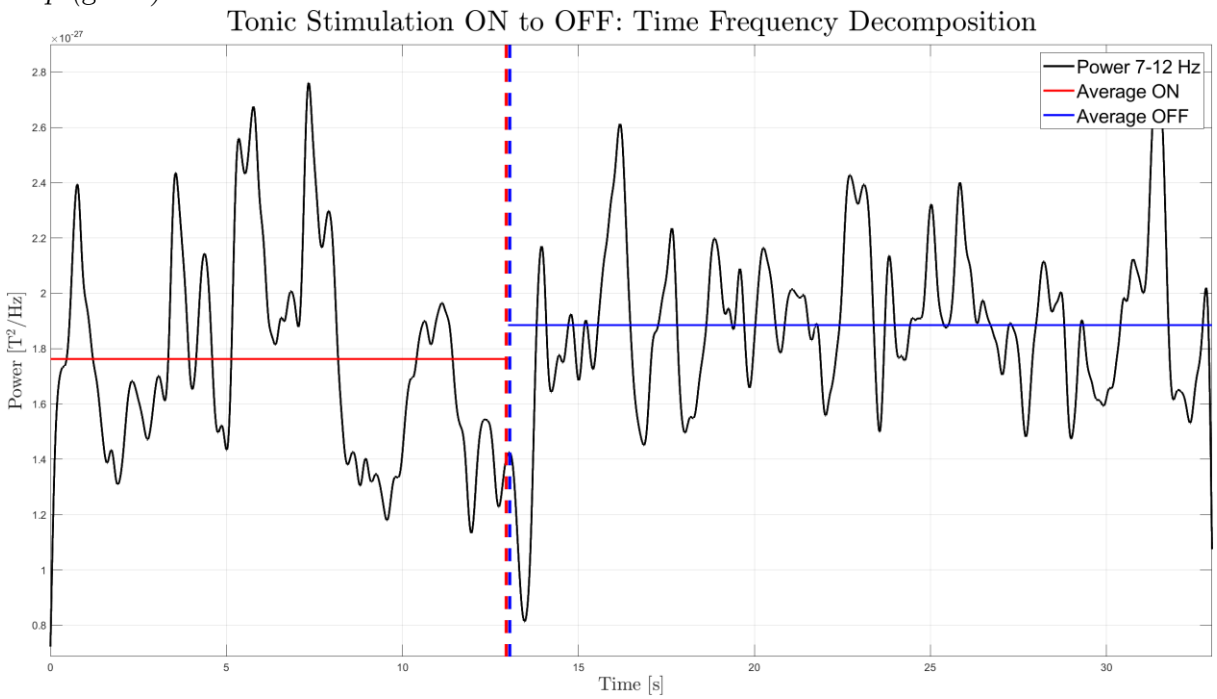

Figure 13: Average power of the 7 – 12 Hz band per time point in the TFD (black), average power during tonic stimulation ON (red) and OFF (blue).

In Figure 14 the TFD of the transition from burst stimulation OFF to ON is shown. The ramp starts at 10 seconds, and the full stimulation starts at 14 seconds (dashed red line). A small decrease in power is visible during the ramp. After the stimulation turned ON, the power in the alpha band was generally higher than in the OFF period.

Figure 15 shows the TFD of the transition from burst stimulation ON to OFF. A decrease in alpha power is visible at 14 seconds, when the stimulation turns off. The alpha power peaks are higher during the ON period compared to OFF.

The Z-score normalisations of these TFDs are shown in Appendix 10.2.

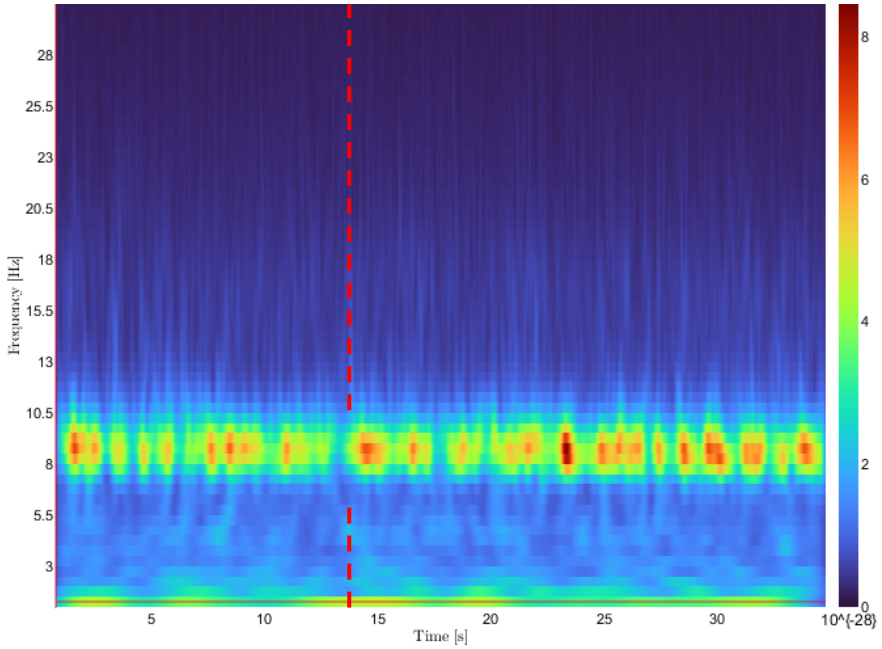

Figure 14: Transition from burst stimulation OFF to ON in PT06: time frequency decomposition. The ramp starts at 10 seconds and the full stimulation starts at 14 seconds (dashed red line).

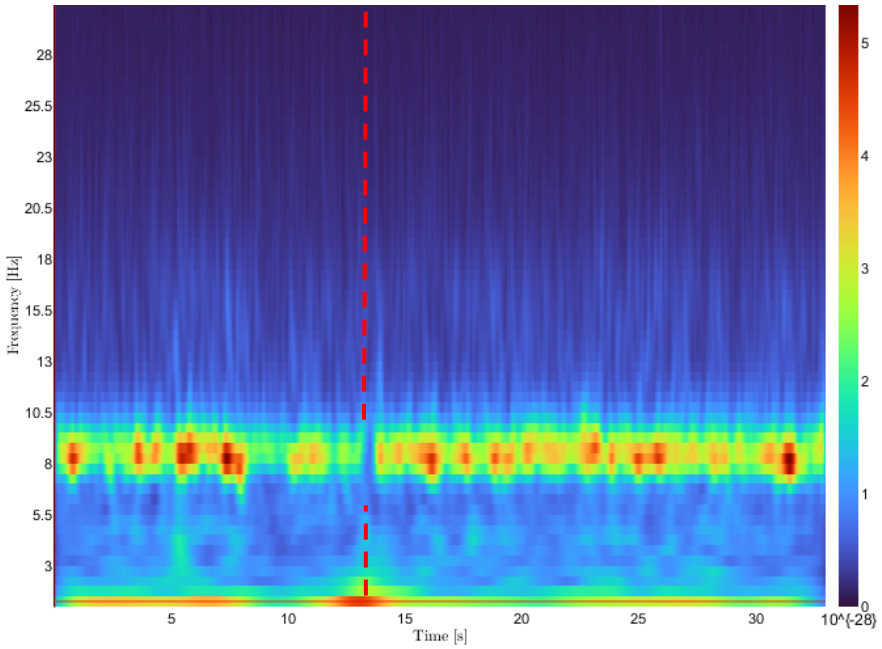

Figure 15: Transition from burst stimulation ON to OFF in PT06: time frequency decomposition. The stimulation stops at 14 seconds (dashed red line).

In Figures 16 and 17 the average alpha power per time point and the average power during stimulation ON, OFF, and the ramp are shown for the transitions during burst stimulation. Figure 16 shows the transition from OFF to ON. The power oscillated on a lower frequency during the ramp, and was increased after the stimulation turned ON. Figure 17 shows the transition from ON to OFF. The ON and OFF segments look identical.

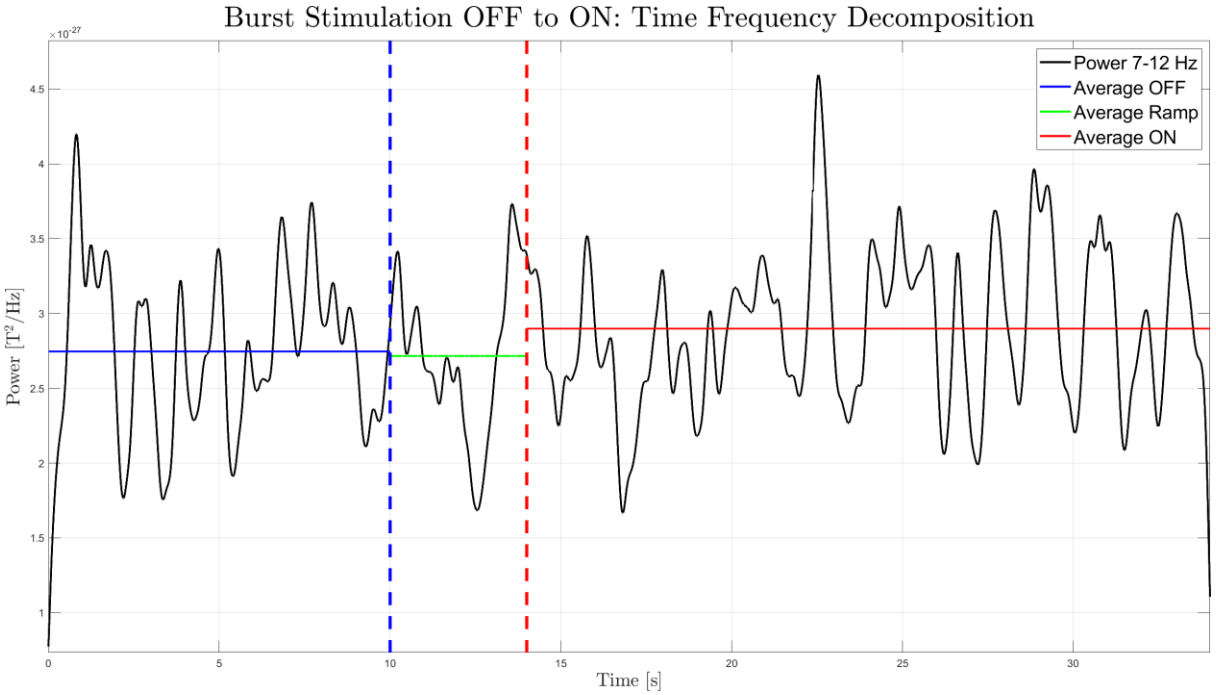

Figure 16: Average power of the 7 – 12 Hz band per time point in the TFD (black), average power during burst stimulation OFF (blue) and ON (red), and the average power during the ramp (green).

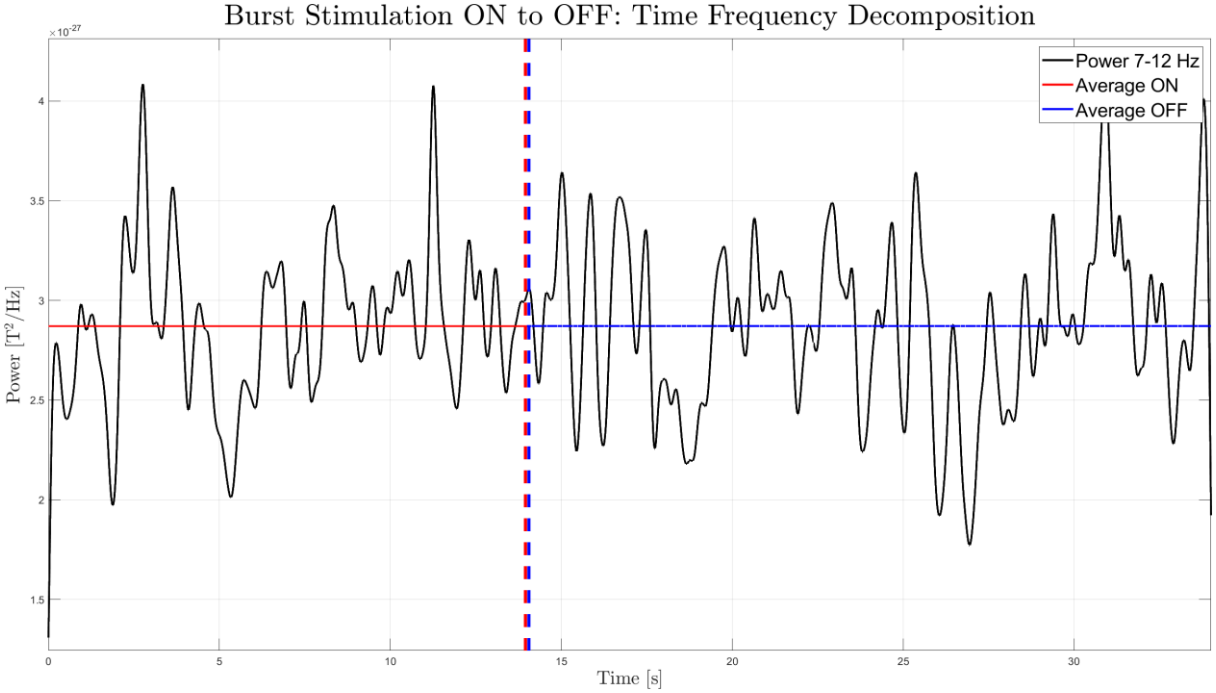

Figure 17: Average power of the 7 – 12 Hz band per time point in the TFD (black), average power during burst stimulation ON (red) and OFF (blue).

6.3 Results: brain regions

The power in the alpha band was equal or lower during tonic ON compared to tonic OFF in all regions. This was most evident in the right thalamus and left S1. The TFDs of these two regions are shown in Figure 18a-d. A decrease in alpha power was visible when the stimulation switched (ON to OFF and OFF to ON). The Z-score transformations are provided in Appendix 10.3.

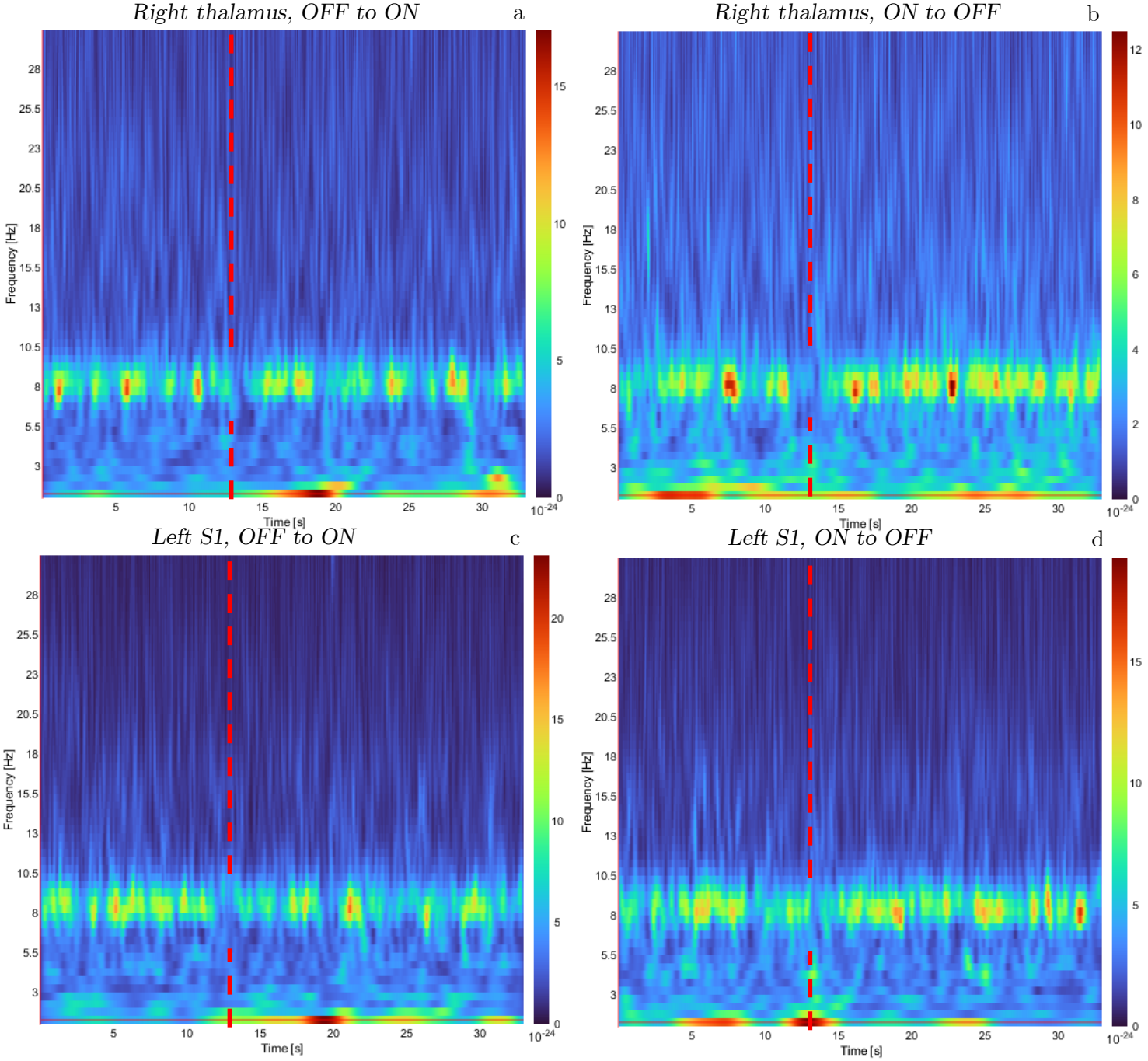

Figure 18a-d: Time frequency decompositions of the transitions (dashed red lines) during tonic stimulation, (a) shows the transition from OFF to ON in the right thalamus, (b) shows the transition ON to OFF in the right thalamus, (c) shows the transition from OFF to ON in the left primary sensory cortex, (d) shows the transition from ON to OFF in the left primary sensory cortex. S1: primary sensory cortex.

Figures 19 and 20 show the average alpha power per time point for the left S1 during tonic stimulation. They show a lower average power during stimulation ON and they show the decrease in power at the transition points. Appendix 10.4 shows these averages for the right thalamus.

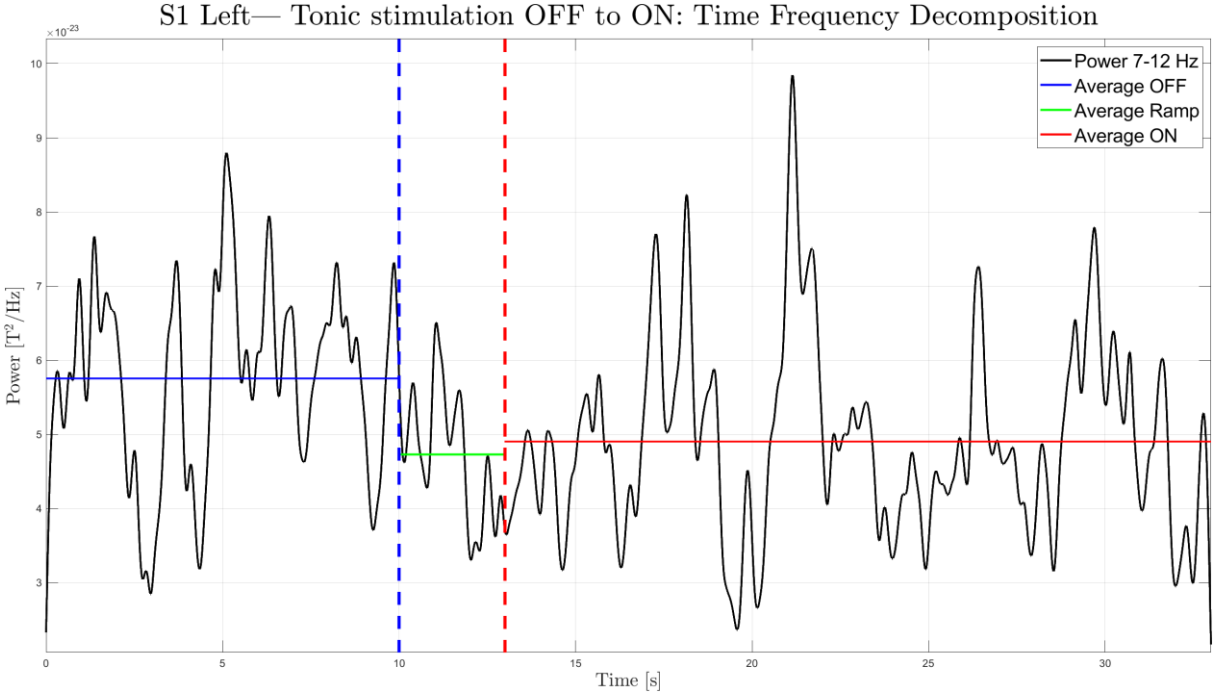

Figure 19: Average power of the 7 – 12 Hz band per time point in the TFD (black), average power during tonic stimulation OFF (blue) and ON (red), and the average power during the ramp (green) in the left primary sensory cortex.

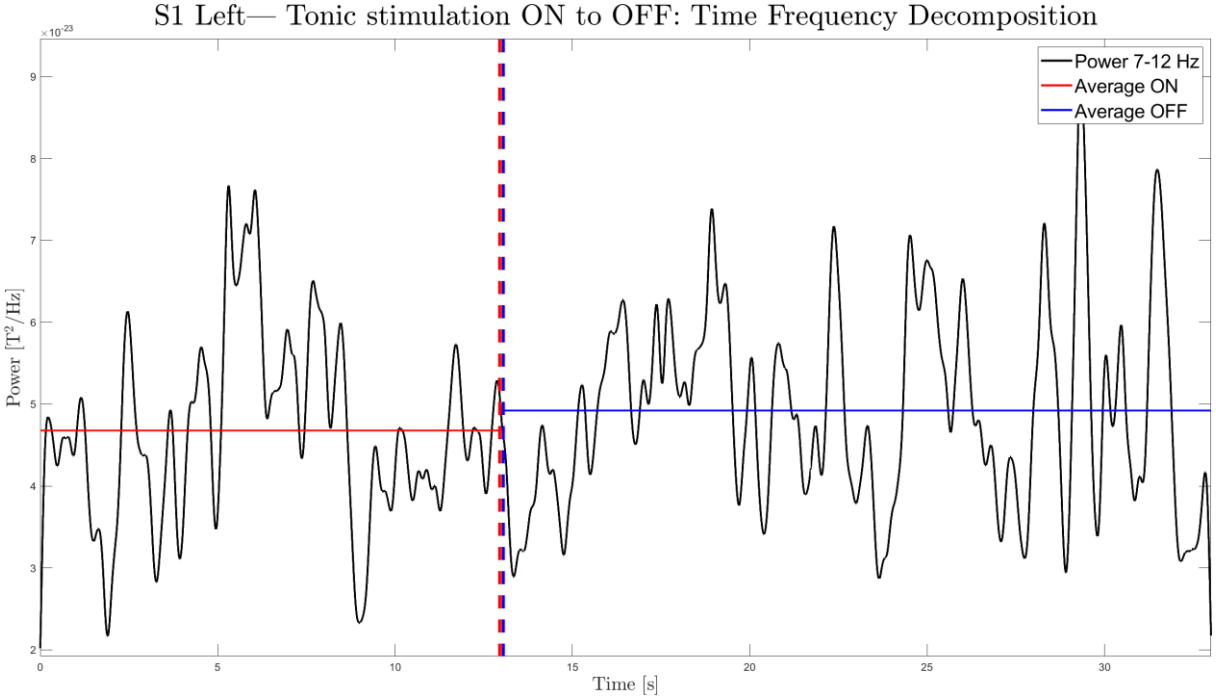

Figure 20: Average power of the 7 – 12 Hz band per time point in the TFD (black) and the average power during tonic stimulation OFF (blue) and ON (red) in the left primary sensory cortex.

The power in the alpha band was equal or increased during burst ON compared to tonic OFF in all regions. This was most evident in the right thalamus and left dlPFC. The TFDs of these two regions are shown in Figure 21a-d. The Z-score transformations are provided in Appendix 10.5.

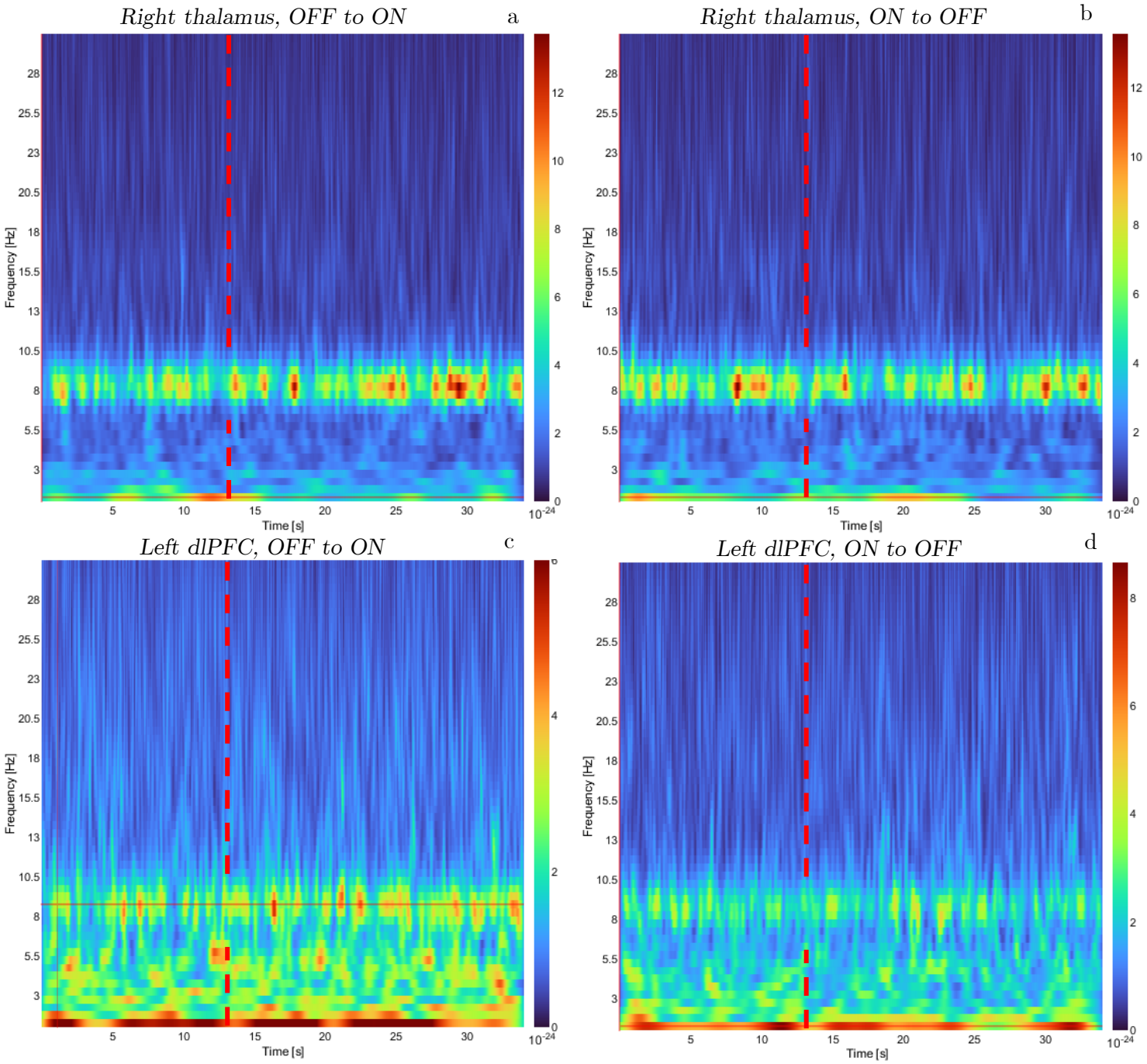

Figure 21a-d: Time frequency decompositions of the transitions (dashed red lines) during burst stimulation, (a) shows the transition from OFF to ON in the right thalamus, (b) shows the transition ON to OFF in the right thalamus, (c) shows the transition from OFF to ON in the left dorsolateral prefrontal cortex, (d) shows the transition from ON to OFF in the left dorsolateral prefrontal cortex. dlPFC: dorsolateral prefrontal cortex.

Figures 22 and 23 show the average alpha power per time point for the left dlPFC during burst stimulation. Figure 22 shows an increased average power when the stimulation turned ON and Figure 23 shows no change in average power when the stimulation turned OFF. Appendix 10.6 shows these averages for the right thalamus.

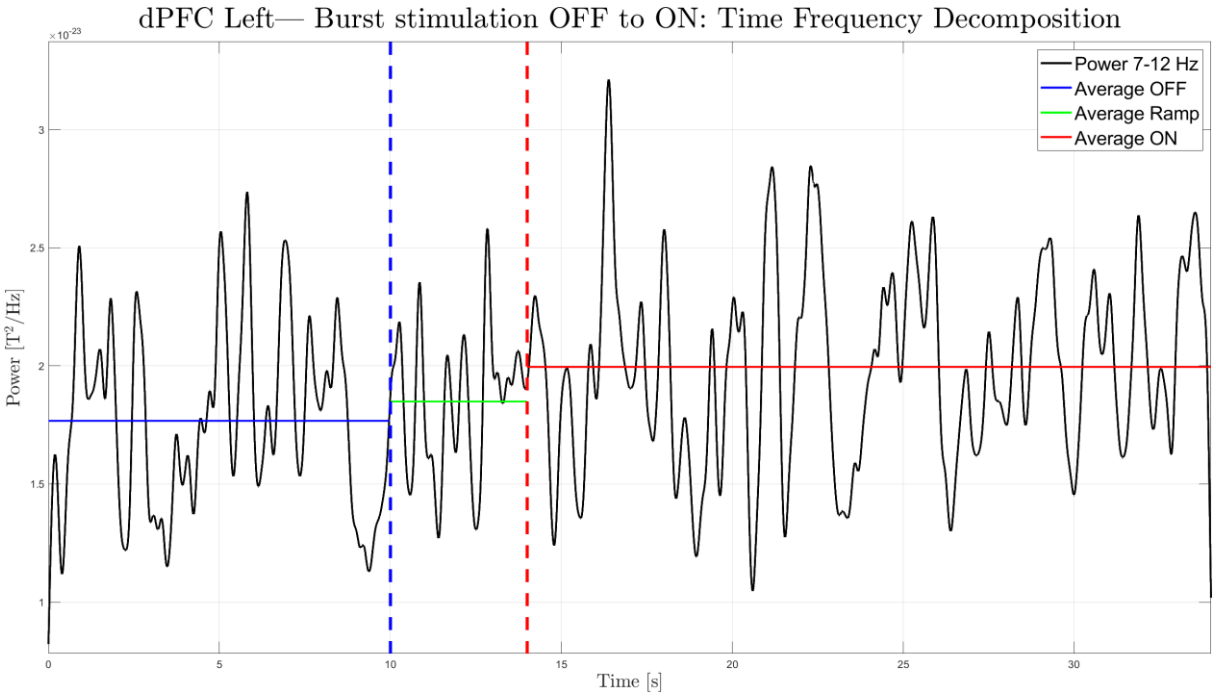

Figure 22: Transition from burst stimulation OFF (blue) to ON (red) in the right thalamus: average power of the 7-12 Hz band.

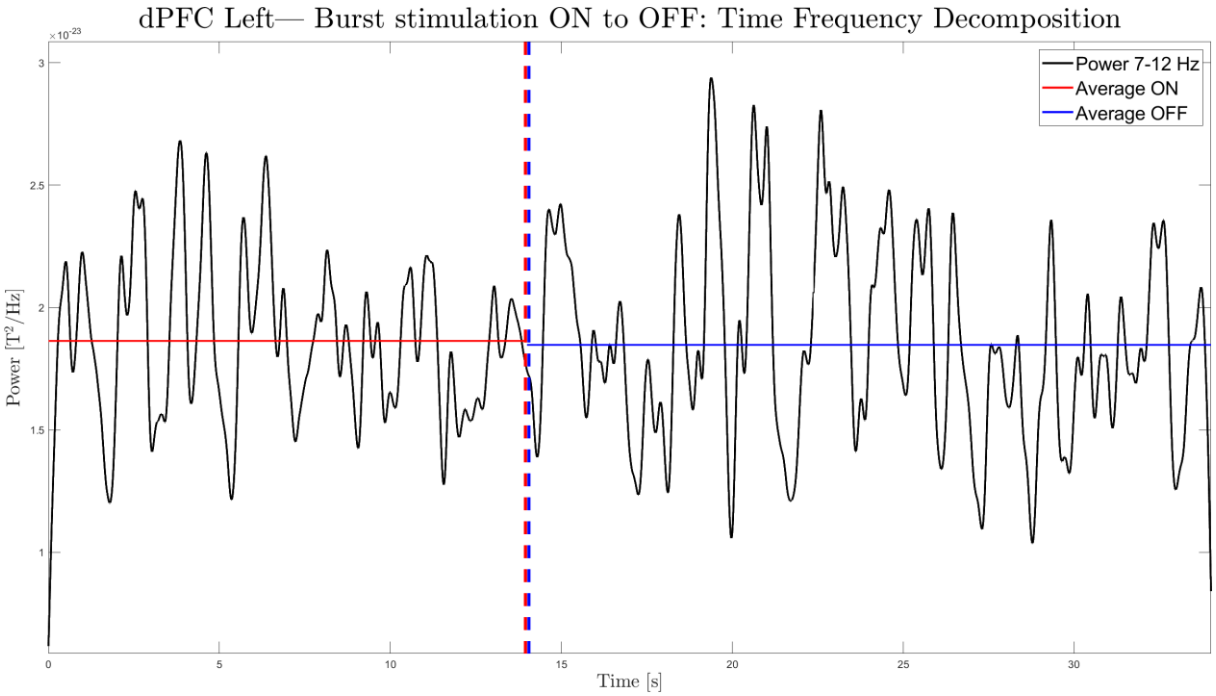

Figure 23: Transition from burst stimulation ON (red) to OFF (blue) in the left dorsolateral prefrontal cortex: average power of the 7-12 Hz band.

7. Discussion

The aim of this study was to image the acute modulation of neuronal activity by SCS treatment in chronic pain patients with MEG. Differences between stimulation ON and OFF as well as differences between tonic and burst stimulation were studied. This was analysed with increasing detail in three different chapters: first the whole brain sensor averages, then the averages of the brain region sources, and lastly the TFD of a single patient.

7.1 Sensor space analysis

In chapter 4 the analysis of the whole brain sensor averages was described. The modulation of three power ratios was studied: Ratio 1: 7-9/9-11 Hz, Ratio 2: 4-7/7-12 Hz, and Ratio 3: 8-10/10-12 Hz.

Ratio 1 and 3 increased during stimulation ON for both tonic and burst stimulation, while Ratio 2 decreased. Although not statistically significant, this suggests that the power shifts from both the 4-7 Hz and the 9-12 Hz ranges towards the 7 – 10 Hz range during stimulation ON. This effect was most evident in Ratio 1 and 2, based on both the effect size and the p-values. The PSDs of stimulation ON all showed a small increase of power around 9 Hz when compared to stimulation OFF. The decrease of Ratio 2 also matches the results of Sufianov et al. They reported that the theta power significantly decreased on a whole brain average after three months of tonic SCS, and related it to dysfunction of the thalamocortical connectivity system as reported by Sarnthein and Jeanmonod {Sufianov et al., 2014, Sarnthein and Jeanmonod, 2008}.

The absolute power of the burst PSDs was higher than the power of the tonic PSDs. The differences between tonic and burst were comparable in both the ON state and the OFF state. This indicates that there could be some lingering effect of the stimulation after it switches OFF, otherwise the ratios in both OFF states would be equal. It is unknown how long this lingering effect remains. For this study, this could imply that the effects of burst stimulation continued during the tonic or placebo stimulation. The order in which the patients received the different types of stimulation would then influence the outcome. This could explain the low NRS scores after placebo stimulation.

If this is indeed the case it makes it very difficult to separate the effects of different types of stimulation. Also, it would bring uncertainty to the results of studies in which different stimulation types are used in a relative short period. More research would be needed to clarify this, as our own data shows no clear pattern. PT04, PT09, and PTN15 showed the most decrease in pain score after placebo stimulation compared to tonic or burst stimulation: PT04 was first set to burst and then to placebo and had equal NRS, PT09 had burst stimulation before placebo but reported more pain during burst than during placebo, and PTN15 first had placebo and also reported more pain during burst. Another possibility would of course be that the placebo stimulation used in this study did have some therapeutic effects.

Even though the four individual patients whose PSDs were analysed all perceived more than 50% pain reduction, the spectral features and modulation were very heterogeneous. This adds to the uncertainty of group level analysis, and supports the idea of multiple mechanisms being involved in the onset of chronic pain. Because of this heterogeneity I decided, in consultation with my supervisors, not to analyse the individual brain regions, because of the variation that was already visible on the sensor level.

7.2 Source space analysis

In chapter 5 the analysis of the brain regions averages were discussed. The largest effects were seen in Ratio 2. Comparing tonic ON and OFF, this ratio decreased in the dlPFC and S1 with a p value of 0.07. This corresponds to the findings of De Ridder and Vanneste, who reported modulation of theta power in S1 during tonic stimulation compared to placebo stimulation, after a week of each stimulation type {De Ridder and Vanneste, 2016}. The theta modulation in S1 was presented as modulation of the lateral pain pathway. They turned the stimulator off completely for the placebo stimulation, making it a clear comparison.

De Ridder and Vanneste also reported modulation of theta power in S1 by burst stimulation. This matches my results, as all three Ratios were increased in S1 during burst stimulation ON compared to OFF. The same comparison for burst stimulation showed a decreased Ratio 2 in the dlPFC, thalamus, and the dACC in the ON state. This matches the results of Witjes et al. (decreased Ratio 2 in the frontal brain during burst stimulation), and De Ridder et al. (increased alpha power in dACC during burst stimulation) {Witjes et al., 2019, De Ridder et al., 2013}.

The ratios were decreased during the burst cycles compared to the tonic cycles, both during the ON and during the OFF segments. This supports the hypothesis that there are lingering effects of burst stimulation after it is switched off, as described in 7.1.

Ratio 2 showed the most evident difference between tonic and burst stimulation, especially in the dlPFC, dACC, insula, and thalamus. Again these findings correspond well to the findings in articles where spectral modulation after longer periods of SCS was studied. De Ridder et al. reported increased alpha power in the dlPFC and the dACC for burst stimulation compared to tonic stimulation {De Ridder et al., 2013}. De Ridder and Vanneste showed modulation of theta band power in the insula when comparing tonic and burst stimulation {De Ridder and Vanneste., 2016}. Lerman et al. reported decreased theta power in the (mediodorsal) thalamus {Lerman et al., 2019}. All three studies attribute these changes to modulation of the medial pain pathway.

7.3 Time frequency decomposition

In chapter 6 the time frequency decompositions of both the sensor and source averages of a single patient were shown. In the tonic TFDs of the whole brain averages, decreases in alpha power were visible at the moment the stimulation switched OFF or ON. This could be caused by the induced paresthesia, as this causes a sudden change in sensation (both when it emerges and when it disappears). The average power in the alpha band was equal or slightly decreased during tonic stimulation ON compared to OFF.

The TFDs of the burst segments showed a decrease in the theta and alpha band power when the stimulation switches ON or OFF. The average power in the ON state increased compared to the OFF state for the burst stimulation. The alpha band power was equal or increased during burst stimulation ON compared to OFF. It is interesting that similar spectral modulations as during tonic stimulation can be seen in the burst TFDs, because burst stimulation does not induce paresthesia. As this patient reported sufficient pain reduction from both tonic and burst stimulation this means that these power decreases could be related to the effectiveness of the stimulation. Because the patients did not score the pain during the cyclic stimulation, it is not possible to relate the amount of decrease in power to the effect of the stimulation.

Similar patterns for tonic and burst stimulation were visible in the TFDs of the various brain regions, like the decrease in power when the stimulation switched ON or OFF. Comparing stimulation ON with OFF, tonic showed equal or lower alpha, while burst showed equal or increased alpha during the ON period.

Changes in V1 were also visible when the stimulation switched, indicating that this region was not suitable as a neutral reference, but it is unclear how V1 is involved in the pain processing. This is however in line with the results of a study by Witjes et al. in which they showed that Ratio 1 significantly changed in several areas of the brain, including V1 {Witjes et al., 2021}. This underlines the complexity of pain processing and the effect of SCS on it.

7.4 Limitations

As this was an explorative study with an aim to generate hypotheses for larger studies, it had some limitations. The limitations can roughly be split in to three areas: the data acquisition, the data processing, and the available literature.

The analyses were limited by the data acquisition because pain scores during the cyclic stimulation were not recorded. Also there was no data of how fast the pain reduction was achieved or when the stimulation was perceived by the individual patients. Because of this it was not possible to distinguish spectral modulation due to changing pain sensation and due to the stimulation itself.

Limitations in data processing involved large artefacts coming from temporal channels in low frequencies after computing the source localisation. This could not be prevented, as it was caused by (dental) implants. Because of this, the power was normalised against the power in the 4-62 Hz band for the sources instead of the 1-62Hz band which was used for the sensor averages. As a result, it is not possible to directly compare the sensor and the source power. Another important limitation were the scout sizes in the AAL atlas. These covered larger

areas than desired, but they could not be changed reliably. An example of the implications of this was that S1 was included as a whole for all patients, instead of only including the part linked to the pain area. This could dilute the effect of the stimulation. Also, regions in both hemispheres were analysed separately from each other, but the side on which the patient experienced pain was not taken into account.

It is inherent to doing experimental research to have little literature available. MEG imaging of long-term modulation of neuronal activity by SCS is a very new field. The lack of comparable studies makes it difficult to substantiate the assumptions made in this study. Only nine full text articles were available for my literature study after also including EEG studies. Of these nine articles only one studied acute neuronal modulation by SCS: Telkes et al. studied the acute modulation of spectral features intra-operatively with EEG {Telkes et al., 2020}. They showed that Ratio 2 decreased in the prefrontal cortex during high frequent (10 kHz) stimulation compared to the baseline recordings. They were unable to correlate these changes with achieved pain relief after implantation.

7.5 Future research

A major topic of interest for future research would be the lingering effect of burst stimulation (and possibly other stimulation types), as the existence of this effect would implicate that the results of previous studies becomes a bit less certain. This could be determined by recording MEG with short time intervals after turning the stimulation OFF, to see when they become similar to the baseline recordings again. Depending on the duration of the stimulation ON period this interval could be a few hours or daily, although this makes it quite burdensome for the patients.

My recommendations for future research would also be to incorporate NRS scores during the MEG recordings in the protocol, and also to quantify how fast each patient perceives changes in pain after stimulation is either turned on or off. Ratio 2 showed the largest effect between ON versus OFF and between tonic versus burst, so I would recommend to incorporate this ratio if spectral features will be analysed.

Because of the large individual differences I would recommend either studying large patient groups, or perform more individual analyses and then group patients who show similar spectral modulation. It would be interesting to compute more TFDs to see if the alpha/theta power drops occur in more patients, and if so, what these patients have in common. When computing these TFDs it could be beneficial to tweak the Morlet wavelet for these specific frequency bands to maximise the spectral resolution with respect to the temporal resolution. That would enable more precise analysis of the ratio modulation over time, something I did not have the time for to include in this report.

8. Conclusion

The primary objective of this TM3 study was to use MEG to analyse the acute effect of burst and tonic SCS on spectral features in the whole brain and in a subset of brain regions. I showed a shift of power to the 7-10 Hz range during tonic and burst stimulation ON, and that burst stimulation modulated the regions involved in the medial pathway more than tonic stimulation did. I also hypothesised that burst stimulation has a lingering effect on the neuronal activity after it is switched OFF.

The secondary objective was to image changes in brain activity during the transition from ON to OFF and vice versa. I showed that alpha power decreased at the moment the stimulation switched ON or OFF.

The results of this study show that acute modulation of brain activity by SCS treatment in chronic pain patients can be detected with MEG, and that this modulation is similar to the results of studies with patients who had longer exposure to SCS. Although most findings were not statistically significant, this shows the possible value of the analysis of acute modulation. There is still room for improvement in SCS treatment, and MEG analysis of acute modulation can help to gain more insight in its working mechanisms.

8. References

[Bruns, 2004]: Andreas Bruns, Fourier-, Hilbert- and wavelet-based signal analysis: are they really different approaches?, Journal of Neuroscience Methods, Volume 137, Issue 2, 2004, Pages 321-332, ISSN 0165-0270, https://doi.org/10.1016/j.jneumeth.2004.03.002.

[Ashburner et al., 2005]: Ashburner J. Friston KJ. Unified segmentation. Neuroimage. 2005;26(3):839-851. doi:10.1016/j.neuroimage.2005.02.018

[Barchini et al., 2012]: Barchini, J., Tchachaghian, S.,Shamaa, F., Jabbur, S., Meyerson, B., Song, Z., Linderoth, B., and Saadé, N. (2012). Spinal segmental and supraspinal mechanisms underlying the pain-relieving effects of spinal cord stimulation: An experimental study in a rat model of neuropathy. Neuroscience, 215:196–208.

[Bentley et al., 2016]: Bentley, L. D., Duarte, R. V., Furlong, P. L., Ashford, R. L., and Raphael, J. H.(2016). Brain activity modifications following spinal cord stimulation for chronic neuropathic pain: A systematic review. Eur J Pain, 20(4):499–511.

[Bonica, 1953]: Bonica JJ. The Management of Pain. Philadelphia. PA: Lea and Febirger; 1953

[Daniell and Osti, 2018]: Daniell JR. Osti OL. Failed Back Surgery Syndrome: A Review Article. Asian Spine J. 2018;12(2):372-379. doi:10.4184/asj.2018.12.2.372

[De Ridder and Vanneste, 2016]: De Ridder, D. and Vanneste, S. (2016). Burst and tonic spinal cord stimulation: Different and common brain mechanisms. Neuromodulation, 19(1):47–59.[Fields, 2004] Fields, H. (2004). State-dependent opioid control of pain. Nature Reviews Neuroscience,5(7):565–575.

[De Ridder et al., 2013]: De Ridder, D., Plazier, M.,Kamerling, N., Menovsky, T., and Vanneste, S.(2013). Burst spinal cord stimulation for limb and back pain. World Neurosurg, 80(5):642–649.

[Hämäläinen, 1991]: Hämäläinen MS. Basic principles of magnetoencephalography. Acta Radiol Suppl. 1991;377:58–62.

[Hämäläinen et al., 1993]: Hämäläinen M. Hari R. Ilmoniemi RJ. Knuutila J. Lounasmaa OV. Magnetoencephalography — Theory. instrumentation. and application to non-invasive studies of the working human brain. Rev Mod Phys. 1993;65:413–97.

[Hämäläinen et al., 1994]: Hämäläinen. M.S.. Ilmoniemi. R.J. Interpreting magnetic fields of the brain: minimum norm estimates. Med. Biol. Eng. Comput. 32. 35–42 (1994)

[Huang et al., 1999]: Huang MX. Mosher JC. Leahy RM (1999) A sensor-weighted overlapping-sphere head model and exhaustive head model comparison for MEG Phys Med Biol. 44:423-440

[Kemler et al., 2000]: Kemler, M. A., Barendse, G. A.,van Kleef, M., de Vet, H. C., Rijks, C. P., Furnée,C. A., and van den Wildenberg, F. A. (2000).Spinal cord stimulation in patients with chronic reflex sympathetic dystrophy. New England Journal of Medicine, 343(9):618–624.

[Kulkarni et al., 2005]: Kulkarni B. Bentley DE. Elliott R. et al. Attention to pain localization and unpleasantness discriminates the functions of the medial and lateral pain systems. Eur J Neurosci. 2005;21(11):3133-3142. doi:10.1111/j.1460-9568.2005.04098.x

[Kumar et al., 2007]: Kumar, K., Taylor, R. S., Jacques,L., Eldabe, S., Meglio, M., Molet, J., Thomson,S., O'Callaghan, J., Eisenberg, E., Milbouw, G.,Buchser, E., Fortini, G., Richardson, J., and North,R. B. (2007). Spinal cord stimulation versus conventional medical management for neuropathic pain: A multicentre randomised controlled trial in patients with failed back surgery syndrome. Pain, 132(1):179–188.

[Leahy et al., 1998]: Leahy RM. Mosher JC. Spencer ME. Huang MX. Lewine JD (1998) A study of dipole localization accuracy for MEG and EEG using a human skull phantom Electroencephalography and Clinical Neurophysiology. 107(2):159-73

[Lerman et al., 2019]: Lerman, I. R., Huang, C., Cui, C.,Xu, L., Gong, Y., Proudfoot, J., Davis, B., Swan,A. R., Angeles, A. M., Rao, R., Baker, D. G., Kim-ball, D., Simmons, A., and Huang, M. (2019). Burstspinal cord stimulation effects on clinical neural cor-relates of pain measured with magnetoencephalogra-phy.Neuromodulation, 22(3):214–216.

[Maihöfner et al., 2010]: Maihöfner C. Seifert F. Markovic K. Complex regional pain syndromes: new pathophysiological concepts and therapies. Eur J Neurol. 2010;17(5):649-660. doi:10.1111/j.1468-1331.2010.02947.x

[Melazack and Wall, 1965]: Melzack R. Wall PD. Pain mechanisms: a new theory. Science. 1965 Nov 19;150(3699):971-9. doi: 10.1126/science.150.3699.971. PMID: 5320816.

[Miller et al., 2016]: Miller JP. Eldabe S. Buchser E. Johanek LM. Guan Y. Linderoth B. Parameters of Spinal Cord Stimulation and Their Role in Electrical Charge Delivery: A Review. Neuromodulation. 2016;19(4):373-384. doi:10.1111/ner.12438

[Moens et al., 2012]: Moens M, Sunaert S, Mariën P, et al. Spinal cord stimulation modulates cerebral function: an fMRI study. Neuroradiology. 2012;54(12):1399-1407. doi:10.1007/s00234-012-1087-8

[Parker et al., 2019]: Parker, T., Huang, Y., Woolrich,M., Aziz, T., and Green, A. (2019). Cortical changesin dorsal root ganglion stimulation.Br J Neurosurg,33(6):707.

[Pizzo et al., 2019]: Pizzo F. Roehri N. Medina Villalon S. et al. Deep brain activities can be detected with magnetoencephalography. Nat Commun. 2019;10(1):971. Published 2019 Feb 27. doi:10.1038/s41467-019-08665-5

[Raja et al., 2020]: Raja. Srinivasa N.a.; Carr. Daniel B.b; Cohen. Miltonc; Finnerup. Nanna B.d.e; Flor. Hertaf; Gibson. Stepheng; Keefe. Francis J.h; Mogil. Jeffrey S.i; Ringkamp. Matthiasj; Sluka. Kathleen A.k; Song. Xue-Junl; Stevens. Bonniem; Sullivan. Mark D.n; Tutelman. Perri R.o; Ushida. Takahirop; Vader. Kyleq The revised International Association for the Study of Pain definition of pain: concepts. challenges. and compromises. PAIN: September 2020 - Volume 161 - Issue 9 - p 1976-1982 doi: 10.1097/j.pain.0000000000001939*

[Sankarasubramanian et al., 2019]: Sankarasubramanian, V., Harte, S. E., Chiravuri, S.,Harris, R. E., Brummett, C. M., Patil, P. G., Clauw,D. J., and Lempka, S. F. (2019). Objective measures to characterize the physiological effects of spinal cord stimulation in neuropathic pain: A literature review. Neuromodulation, 22(2):127–148.

[Sarnthein and Jeanmonod, 2008]: Sarnthein, J. and Jeanmonod, D. (2008). High thalamocortical theta coherence in patients with neurogenic pain. NeuroImage, 39(4):1910–1917.

[Schulman et al., 2005]: Schulman, J. J., Ramirez,R. R., Zonenshayn, M., Ribary, U., and Llinas, R.(2005). Thalamocortical dysrhythmia syndrome: Meg imaging of neuropathic pain. Thalamus Relat Syst,3(1):33–39.

[Sears et al., 2011]: Sears, N. C., Machado, A. G., Nagel ,S. J., Deogaonkar, M., Stanton-Hicks, M., Rezai,A. R., and Henderson, J. M. (2011). Long-term out-comes of spinal cord stimulation with paddle leads in the treatment of complex regional pain syndrome and failed back surgery syndrome. Neuromodulation: Technology at the Neural Interface, 14(4):312–318.

[Shealy et al, 1967]: Shealy CN. Mortimer JT. Reswick JB. Electrical inhibition of pain by stimulation of the dorsal columns: preliminary clinical report. Anesth Analg. 1967;46(4):489-491.

[Singh, 2014]: Singh SP. Magnetoencephalography: Basic principles. Annals of Indian Academy of Neurology. 2014 Mar;17(Suppl 1):S107-12. DOI: 10.4103/0972-2327.128676.

[Squire et al., 2008]: Squire, L., Berg, D., Bloom, F., du Lac, S., Ghosh, A., and Spitzer, N. (2008). Fundamental Neuroscience, Chapter 25 Somatosensory System. Academia Press, Amsterdam, 3rd edition.

[Sufianov et al., 2014]: Sufianov, A. A., Shapkin, A. G.,Sufianova, G. Z., Elishev, V. G., Barashin, D. A.,Berdichevskii, V. B., and Churkin, S. V. (2014). Functional and metabolic changes in the brain in neuropathic pain syndrome against the background of chronic epidural electrostimulation of the spinal cord. Bull Exp Biol Med, 157(4):462–465.

[Tadel et al., 2011]: Tadel F, Baillet S, Mosher JC, Pantazis D, Leahy RM (2011) Brainstorm: A User-Friendly Application for MEG/EEG Analysis Computational Intelligence and Neuroscience, vol. 2011, Article ID 879716, 13 pages, 2011. doi:10.1155/2011/879716

[Taylor et al., 2013]: Taylor, R. S., Desai, M. J.,Rigoard, P., and Taylor, R. J. (2013). Predictors of pain relief following spinal cord stimulation in chronic back and leg pain and failed back surgery syndrome: A systematic review and meta-regression analysis. Pain Practice, 14(6):489–505

[Telkes et al., 2020]: Telkes, L., Hancu, M., Paniccioli,S., Grey, R., Briotte, M., McCarthy, K., Raviv, N.,and Pilitsis, J. G. (2020). Differences in eeg patterns between tonic and high frequency spinal cord stimulation in chronic pain patients. Clin Neurophysiol,131(8):1731–1740.

[Tesche et al., 1995]: Tesche CD. Uusitalo MA. Ilmoniemi RJ. Huotilainen M. Kajola M. Salonen O. Signal-space projections of MEG data characterize both distributed and well-localized neuronal sources. Electroencephalogr Clin Neurophysiol. 1995;95(3):189-200. doi:10.1016/0013-4694(95)00064-6

[Turk et al., 2011]: Turk DC. Wilson HD. Cahana A. Treatment of non-cancer pain. Lancet. 2011;377(9784):2226–2235.

[Tzourio-Mazoyer et al., 2002]: Tzourio-Mazoyer. B. Landeau. D. Papathanassiou. F. Crivello. O. Etard. N. Delcroix. B. Mazoyer. M. Joliot. Automated Anatomical Labeling of Activations in SPM Using a Macroscopic Anatomical Parcellation of the MNI MRI Single-Subject Brain. NeuroImage. Volume 15. Issue 1. 2002. Pages 273-289. ISSN 1053-8119

[Uusitalo et al., 1997]: Uusitalo MA. Ilmoniemi RJ. Signal-space projection method for separating MEG or EEG into components. Med Biol Eng Comput. 1997;35(2):135-140. doi:10.1007/BF02534144

[Witjes et al., 2019]: Witjes, B., De Vos, C., Roy, M.,Bock, E., Oostenveld, R., and Baillet, S. (2019).Magneto-encephalography (meg) to image the brain's role in the analgesic effects of spinal cord stimulation(scs). Neuromodulation, 22(2):39.

[Witjes et al., 2021]: Witjes, B., Baillet, S., Roy, M., Oostenveld, R., Huygen, F., De Vos, C. (2021). Magnetoencephalography reveals increased slow-to-fast alpha power ratios in patients with chronic pain. PAIN Reports, [Accepted].

9. Appendix

10.1 Individual PSDs

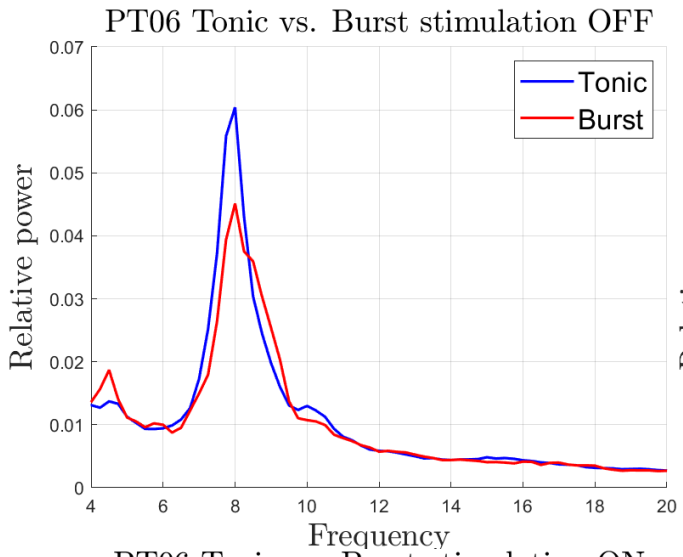

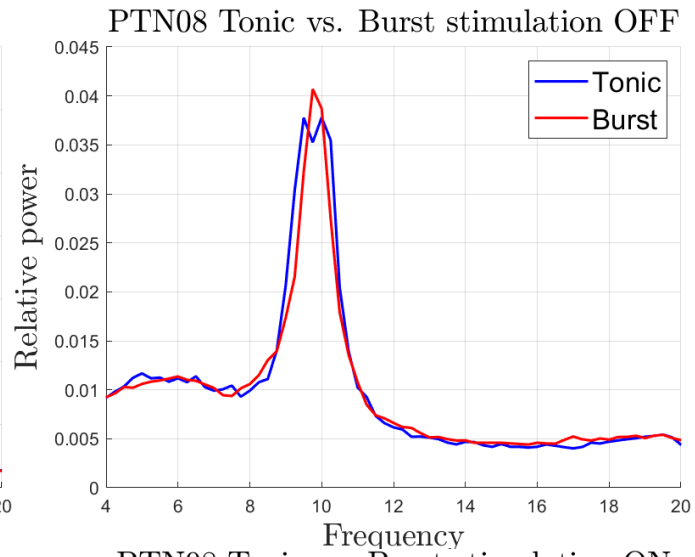

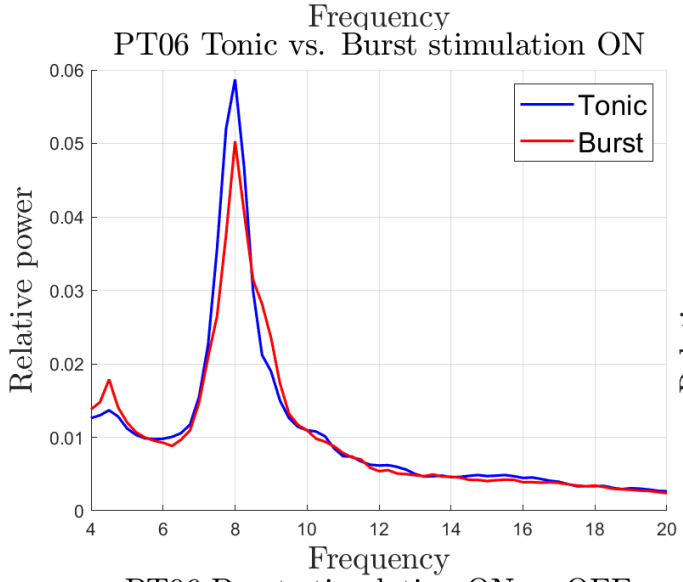

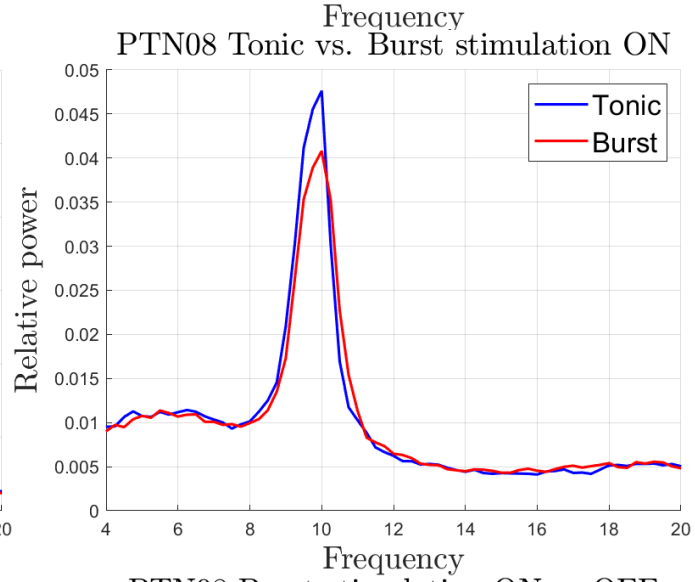

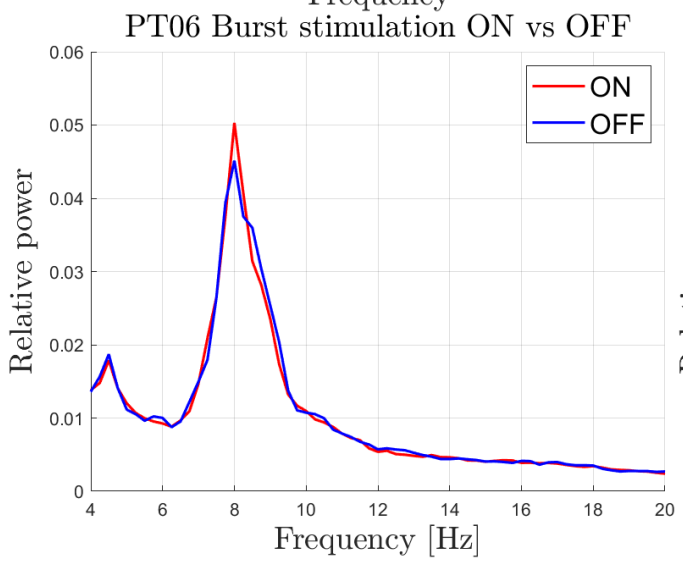

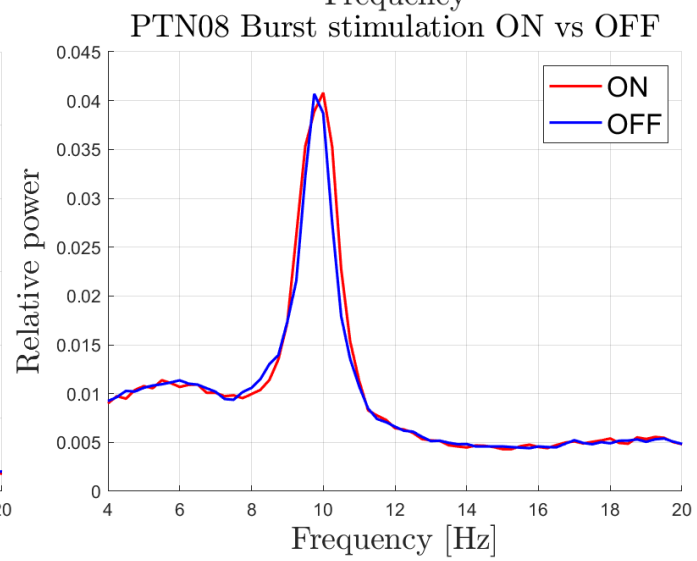

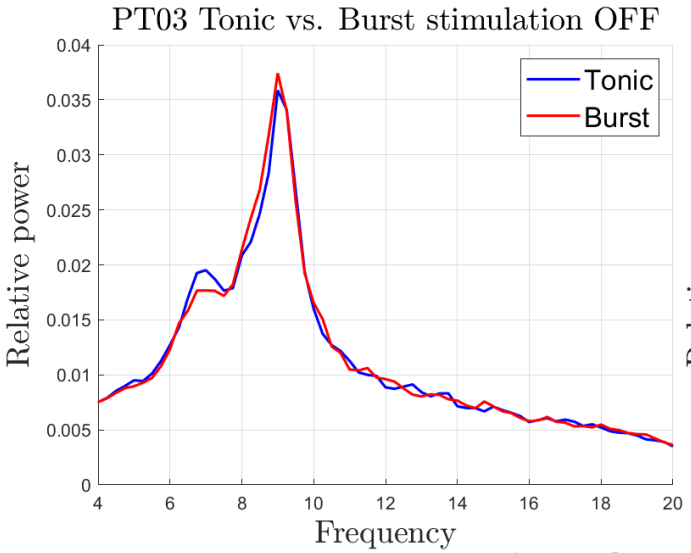
PT03 Tonic vs. Burst stimulation OFF
Tonic
Burst
Relative power
Frequency

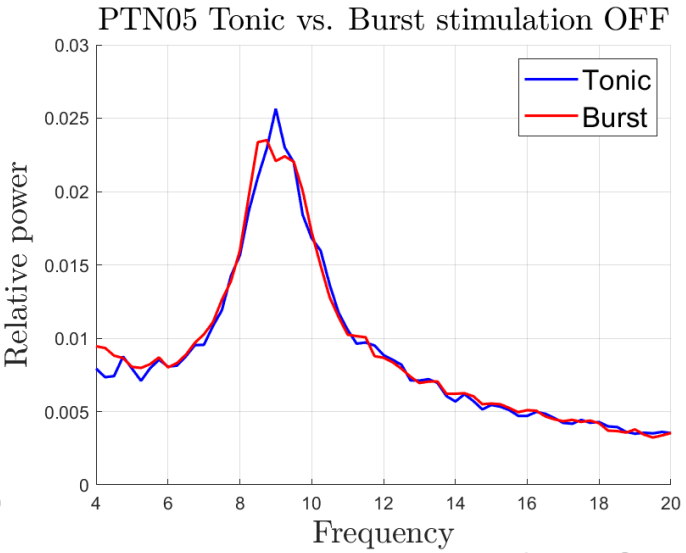
PTN05 Tonic vs. Burst stimulation OFF
Tonic
Burst
Relative power
Frequency

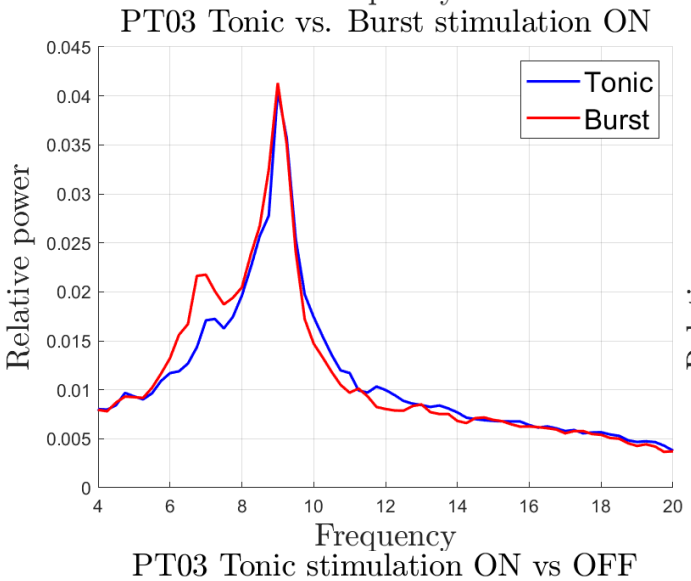
PT03 Tonic vs. Burst stimulation ON
Tonic
Burst
Relative power
Frequency

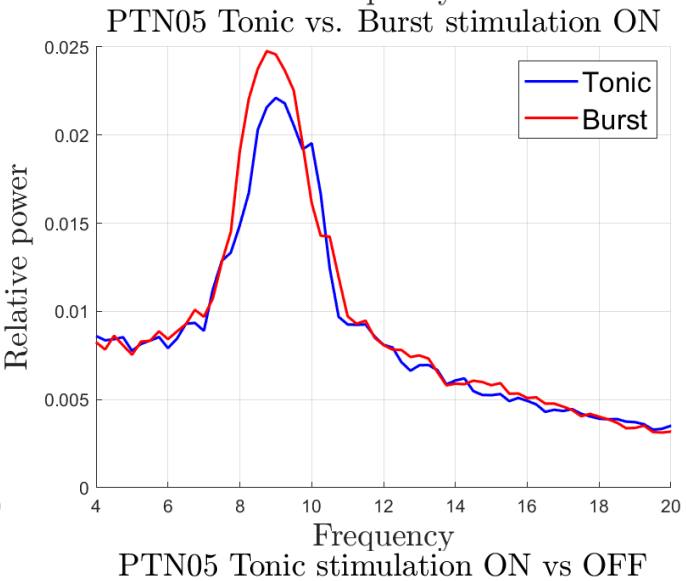
PTN05 Tonic vs. Burst stimulation ON
Tonic
Burst
Relative power
Frequency

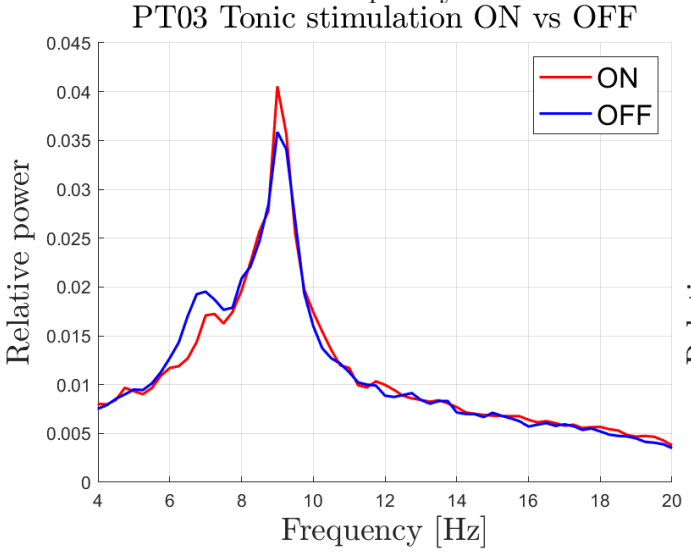
PT03 Tonic stimulation ON vs OFF
ON
OFF
Relative power
Frequency [Hz]

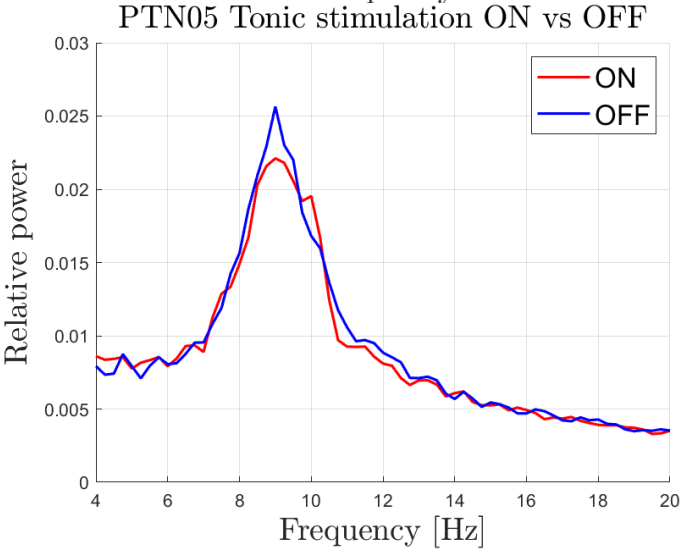
PTN05 Tonic stimulation ON vs OFF
ON
OFF
Relative power
Frequency [Hz]

10.2 Z-score transformations burst stimulation sensor average

In Figure 24 the Z scores of the TFD of the transition from burst stimulation OFF to ON are shown. The alpha power noticeably increased after burst stimulation started, with Z scores between 1 and 4.

In Figure 25 the Z scores of the TFD of the transition from burst stimulation ON to OFF are shown. Theta activity loses some power after the stimulation turns OFF, but the alpha power showed similar oscillations before and after the transition.

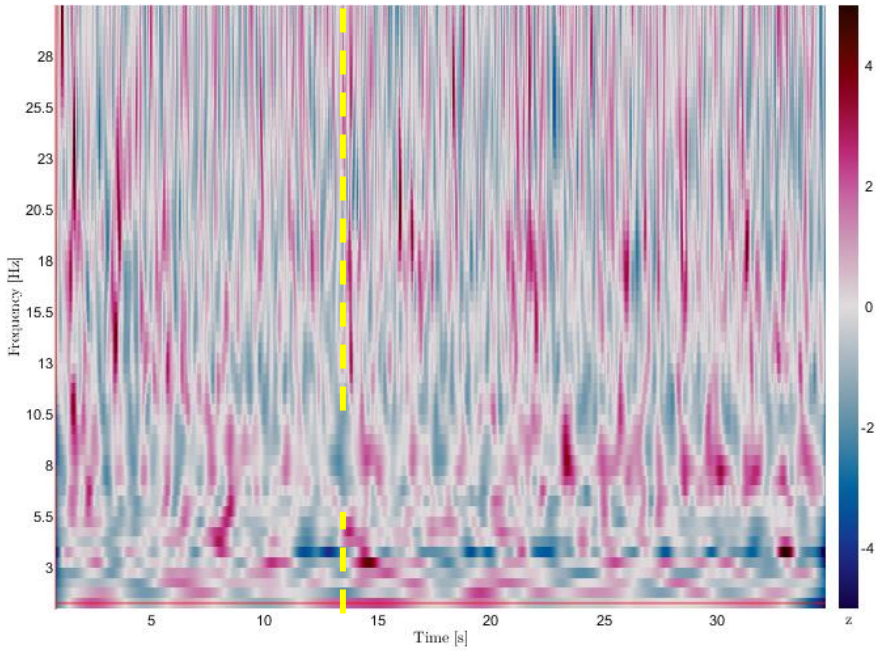

Figure 24: Transition from burst stimulation OFF to ON in PT06: Z-scores of the time frequency decomposition. The ramp starts at 10 seconds and the full stimulation starts at 14 seconds (dashed yellow line).

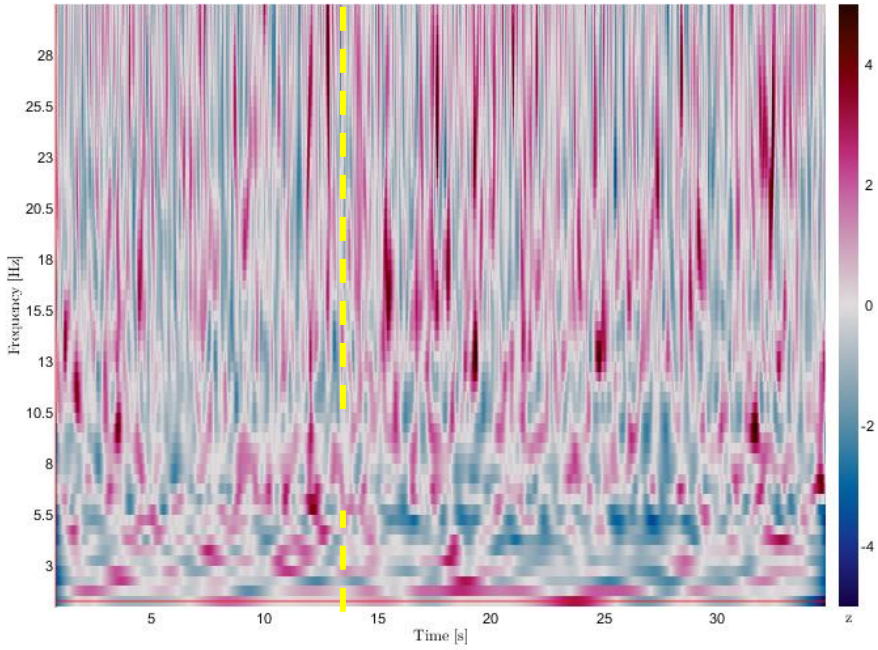

Figure 25: Transition from burst stimulation ON to OFF in PT06: Z-scores of the time frequency decomposition. The stimulation stops at 14 seconds (dashed yellow line).

10.3 Z-score transformations of the tonic stimulation source averages TFDs

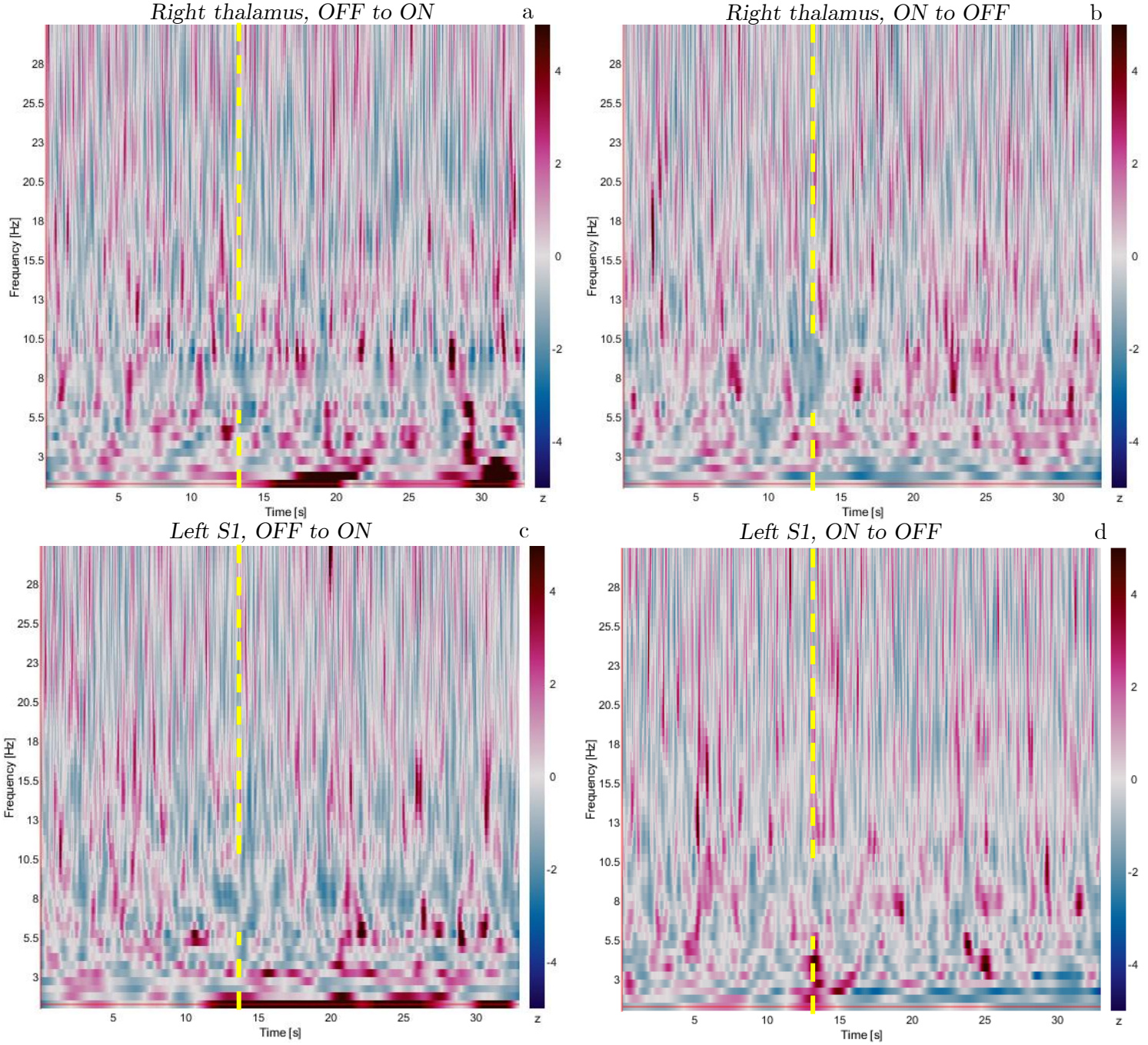

Figure 26: Z-scores of the transitions during tonic stimulation (yellow dashed lines), (a) shows the transition from OFF to ON in the right thalamus, (b) shows the transition ON to OFF in the right thalamus, (c) shows the transition from OFF to ON in the left primary sensory cortex, (d) shows the transition from ON to OFF in the left primary sensory cortex. S1: primary sensory cortex

10.4 Average alpha power per time point, tonic stimulation, right thalamus

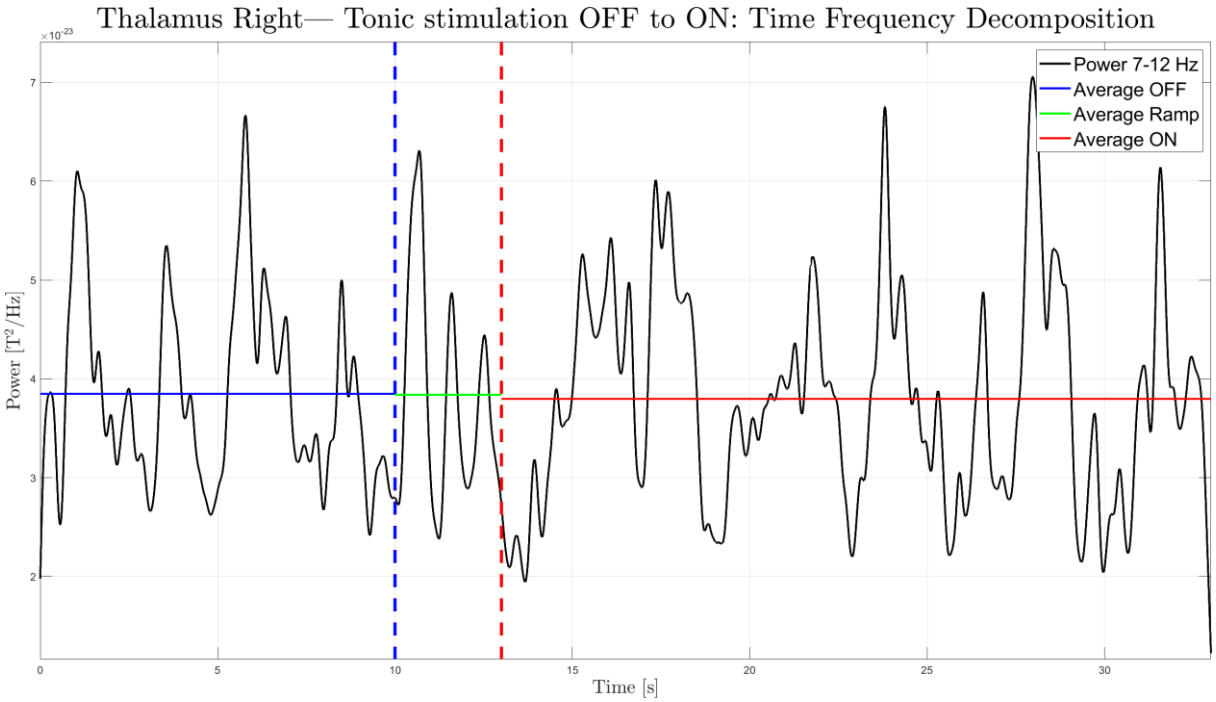

Figure 27: Average power of the 7 – 12 Hz band per time point in the TFD (black), average power during tonic stimulation OFF (blue) and ON (red), and the average power during the ramp (green) in the right thalamus.

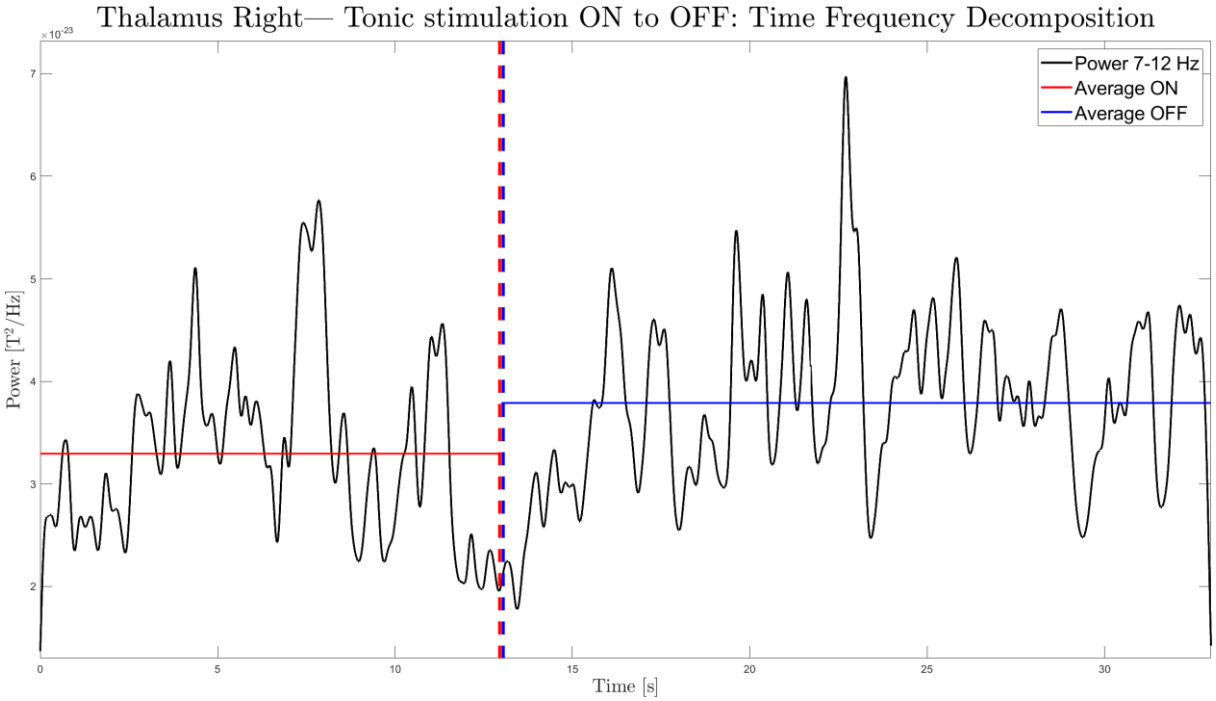

Figure 28: Average power of the 7 – 12 Hz band per time point in the TFD (black) and the average power during tonic stimulation OFF (blue) and ON (red) in the right thalamus.

10.5 Z-score transformations of the burst stimulation source averages TFDs

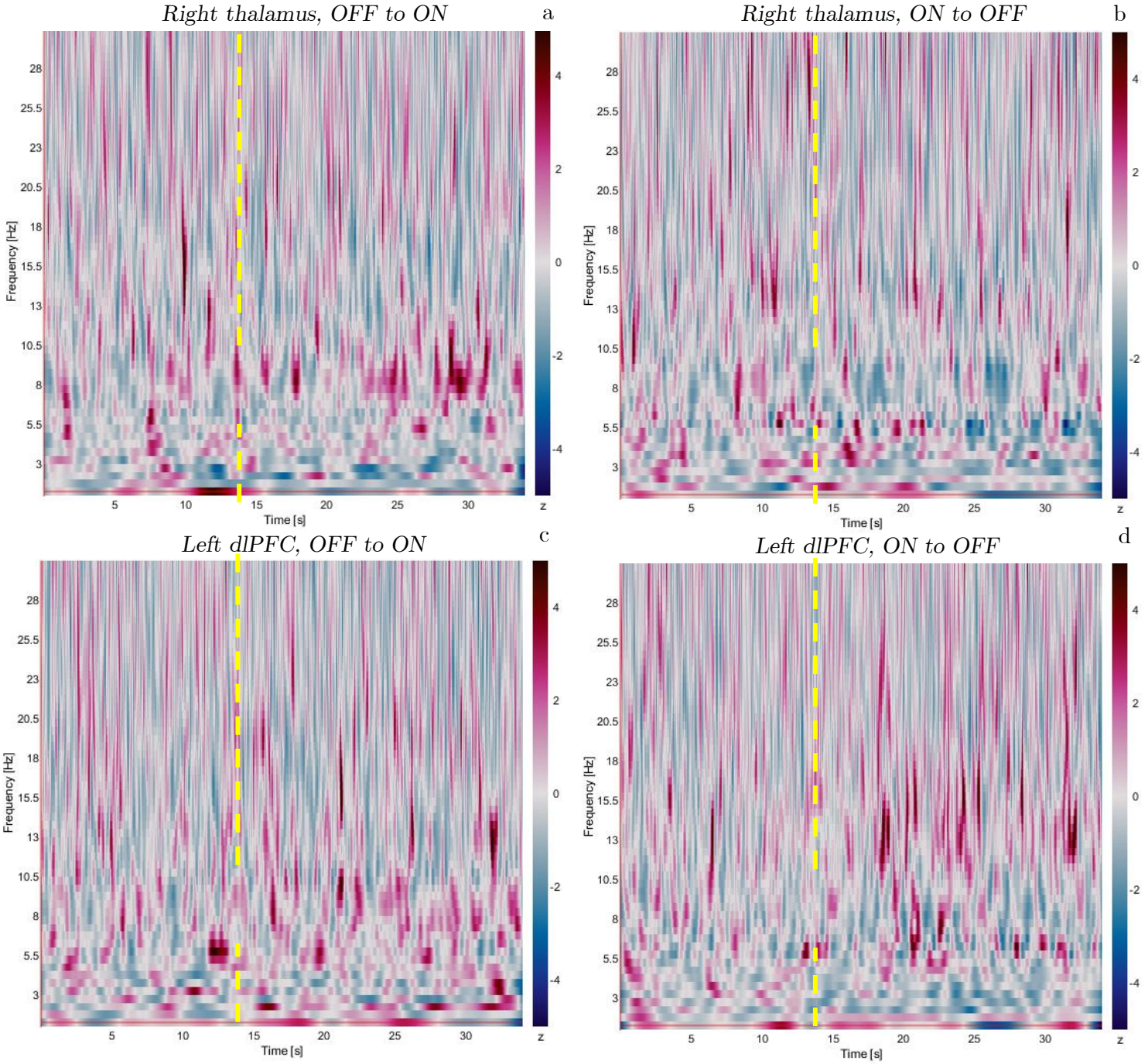

Figure 29: Transitions (yellow dashed lines) from burst stimulation OFF to ON (A,C) and ON to OFF (B,D) in the right thalamus (A and B) and left dorsolateral prefrontal cortex (C and D): Z scores of the time frequency decompositions. dlPFC: dorsolateral prefrontal cortex.

10.6 Average alpha power per time point, burst stimulation, right thalamus

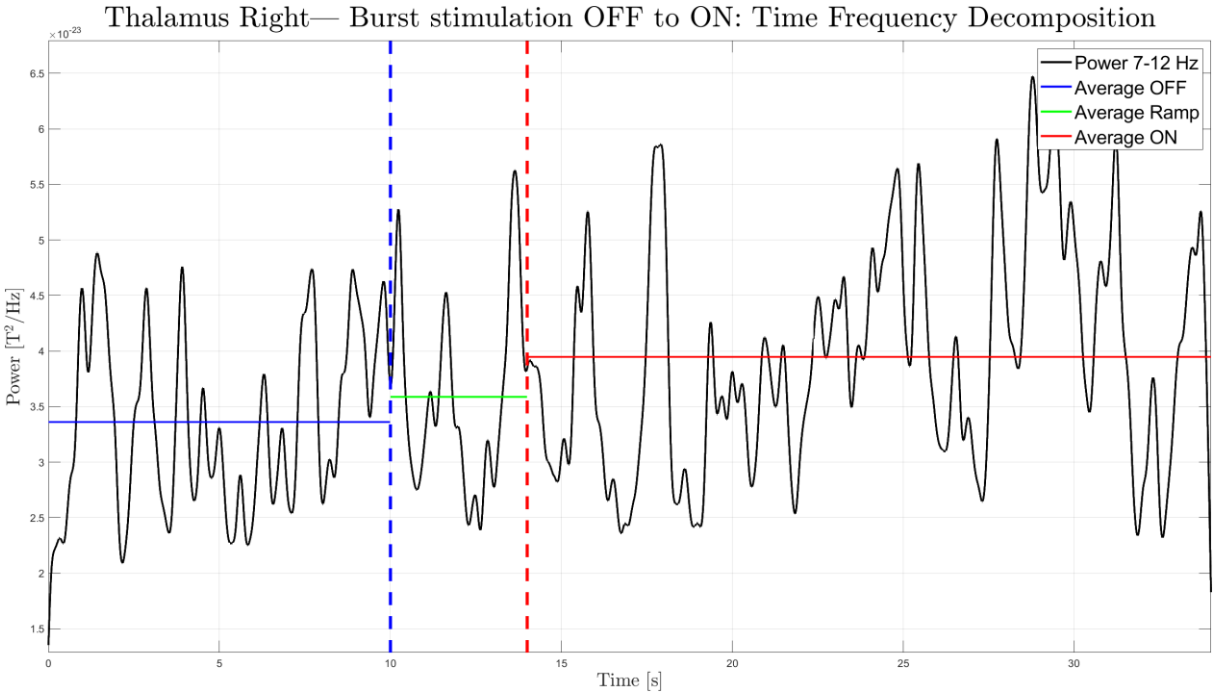

Figure 30: Transition from burst stimulation OFF (blue) to ON (red) in the right thalamus: average power of the 7-12 Hz band.

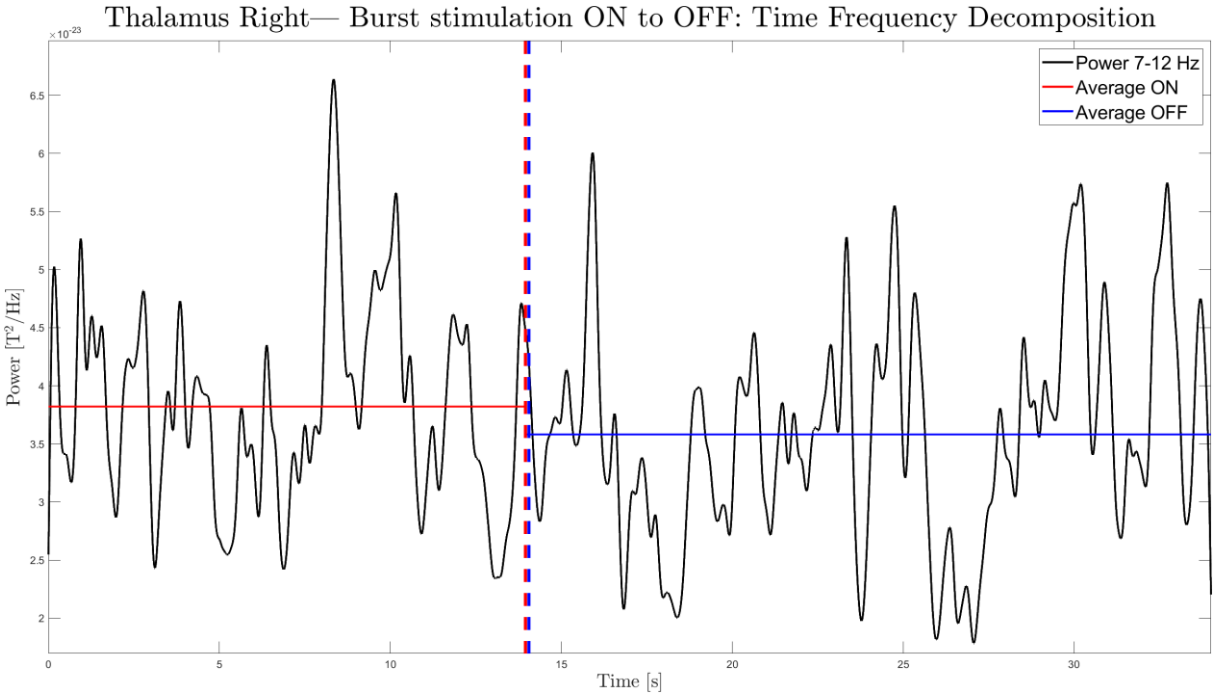

Figure 31: Transition from burst stimulation ON (red) to OFF (blue) in the right thalamus: average power of the 7-12 Hz band.